22 Kufrin D, Eslin DE, Bdeir K, Murciano JC, Kuo A, Kowalska MA, Degen JL, Sachais BS, Cines DB, Poncz M: Antithrombotic thrombocytes: ectopic expression of urokinase-type plasminogen activator in platelets. Blood 2003;102:926–933.
23 Yarovoi HV, Kufrin D, Eslin DE, Thornton MA, Haberichter SL, Shi Q, Zhu H, Camire R, Fakharzadeh SS, Kowalska MA, Wilcox DA, Sachais BS, Montgomery RR, Poncz M: Factor VIII ectopically expressed in platelets: efficacy in hemophilia A treatment. Blood 2003;102:4006–4013.
24 Shi Q, Wilcox DA, Fahs SA, Weiler H, Wells CW, Cooley BC, Desai D, Morateck PA, Gorski J, Montgomery RR: Factor VIII ectopically targeted to platelets is therapeutic in hemophilia A with high-titer inhibitory antibodies. J Clin Invest 2006; 116:1974–1982.
25 Nguyen HG, Yu G, Makitalo M, Yang D, Xie HX, Jones MR, Ravid K: Conditional overexpression of transgenes in megakaryocytes and platelets in vivo. Blood 2005;106:1559–1564.
26 Tiedt R, Schomber T, Hao-Shen H, Skoda RC: Pf4-Cre transgenic mice allow the generation of lineage-restricted gene knockouts for studying megakaryocyte and platelet function in vivo. Blood 2007; 109:1503–1506.
27 Wilcox DA, White GC Jr: Gene therapy for platelet disorders: studies with Glanzmann's thrombasthenia. J Thromb Haemost 2003;1:2300–2311.
28 Kohn DB: Gene therapy using hematopoietic stem cells. Curr Opin Mol Ther 1999;1:437–442.
29 Kohn DB, Sadelain M, Dunbar C, Bodine D, Kiem HP, Candotti F, Tisdale J, Riviere I, Blau CA, Richard RE, Sorrentino B, Nolta J, Malech H, Brenner M, Cornetta K, Cavagnaro J, High K, Glorioso J: American Society of Gene Therapy (ASGT) ad hoc subcommittee on retroviral-mediated gene transfer to hematopoietic stem cells. Mol Ther 2003;8:180–187.
30 Irion R: American Astronomical Society meeting. Snapshots from the meeting. Science 2005;308: 1733.
31 Somia N, Verma IM: Gene therapy: trials and tribulations. Nat Rev Genet 2000;1:91–99.
32 Richter J: Gene transfer to hematopoietic cells – the clinical experience. Eur J Haematol 1997;59: 67–75.
33 Miller DG, Adam MA, Miller AD: Gene transfer by retrovirus vectors occurs only in cells that are actively replicating at the time of infection. Mol Cell Biol 1990;10:4239–4242.
34 Naldini L, Blomer U, Gallay P, Ory D, Mulligan R, Gage FH, Verma IM, Trono D: In vivo gene delivery and stable transduction of nondividing cells by a lentiviral vector. Science 1996;272:263–267.
35 Naldini L: Lentiviruses as gene transfer agents for delivery to non-dividing cells. Curr Opin Biotechnol 1998;9:457–463.
36 Kafri T, Blomer U, Peterson DA, Gage FH, Verma IM: Sustained expression of genes delivered directly into liver and muscle by lentiviral vectors. Nat Genet 1997;17:314–317.
37 Imren S, Fabry ME, Westerman KA, Pawliuk R, Tang P, Rosten PM, Nagel RL, Leboulch P, Eaves CJ, Humphries RK: High-level beta-globin expression and preferred intragenic integration after lentiviral transduction of human cord blood stem cells. J Clin Invest 2004;114:953–962.
38 Puthenveetil G, Scholes J, Carbonell D, Qureshi N, Xia P, Zeng L, Li S, Yu Y, Hiti AL, Yee JK, Malik P: Successful correction of the human beta-thalassemia major phenotype using a lentiviral vector. Blood 2004;104:3445–3453.
39 Woods NB, Ooka A, Karlsson S: Development of gene therapy for hematopoietic stem cells using lentiviral vectors. Leukemia 2002;16:563–569.
40 Pfeifer A, Ikawa M, Dayn Y, Verma IM: Transgenesis by lentiviral vectors: lack of gene silencing in mammalian embryonic stem cells and preimplantation embryos. Proc Natl Acad Sci U S A 2002;99: 2140–2145.
41 Shayakhmetov DM, Carlson CA, Stecher H, Li Q, Stamatoyannopoulos G, Lieber A: A high-capacity, capsid-modified hybrid adenovirus/adeno-associated virus vector for stable transduction of human hematopoietic cells. J Virol 2002;76:1135–1143.
42 Zhong L, Li W, Li Y, Zhao W, Wu J, Li B, Maina N, Bischof D, Qing K, Weigel-Kelley KA, Zolotukhin I, Warrington KH, Jr., Li X, Slayton WB, Yoder MC, Srivastava A: Evaluation of primitive murine hematopoietic stem and progenitor cell transduction in vitro and in vivo by recombinant adeno-associated virus vector serotypes 1 through 5. Hum Gene Ther 2006;17:321–333.
43 Dull T, Zufferey R, Kelly M, Mandel RJ, Nguyen M, Trono D, Naldini L: A third-generation lentivirus vector with a conditional packaging system. J Virol 1998;72:8463–8471.
44 Nakajima T, Nakamaru K, Ido E, Terao K, Hayami M, Hasegawa M: Development of novel simian immunodeficiency virus vectors carrying a dual gene expression system. Hum Gene Ther 2000;11: 1863–1874.
45 Morris KV, Rossi JJ: Anti-HIV-1 gene expressing lentiviral vectors as an adjunctive therapy for HIV-1 infection. Curr HIV Res 2004;2:185–191.
46 Kimura A, Ohmori T, Ohkawa R, Madoiwa S, Mimuro J, Murakami T, Kobayashi E, Hoshino Y, Yatomi Y, Sakata Y: Essential roles of sphingosine 1-phosphate/S1P1 receptor axis in the migration of neural stem cells toward a site of spinal cord injury. Stem Cells 2007;25:115–124.
47 Van Maele B, De Rijck J, De Clercq E, Debyser Z: Impact of the central polypurine tract on the kinetics of human immunodeficiency virus type 1 vector transduction. J Virol 2003;77:4685–4694.
48 Manganini M, Serafini M, Bambacioni F, Casati C, Erba E, Follenzi A, Naldini L, Bernasconi S, Gaipa G, Rambaldi A, Biondi A, Golay J, Introna M: A human immunodeficiency virus type 1 pol gene-derived sequence (cPPT/CTS) increases the efficiency of transduction of human nondividing monocytes and T lymphocytes by lentiviral vectors. Hum Gene Ther 2002;13:1793–1807.
49 Sanders DA: No false start for novel pseudotyped vectors. Curr Opin Biotechnol 2002;13:437–442.
50 Hanawa H, Kelly PF, Nathwani AC, Persons DA, Vandergriff JA, Hargrove P, Vanin EF, Nienhuis AW: Comparison of various envelope proteins for their ability to pseudotype lentiviral vectors and transduce primitive hematopoietic cells from human blood. Mol Ther 2002;5:242–251.
51 Kahl CA, Pollok K, Haneline LS, Cornetta K: Lentiviral vectors pseudotyped with glycoproteins from Ross River and vesicular stomatitis viruses: variable transduction related to cell type and culture conditions. Mol Ther 2005;11:470–482.
52 Kang Y, Xie L, Tran DT, Stein CS, Hickey M, Davidson BL, McCray PB Jr: Persistent expression of factor VIII in vivo following nonprimate lentiviral gene transfer. Blood 2005;106:1552–1558.
53 Bartosch B, Bukh J, Meunier JC, Granier C, Engle RE, Blackwelder WC, Emerson SU, Cosset FL, Purcell RH: In vitro assay for neutralizing antibody to hepatitis C virus: evidence for broadly conserved neutralization epitopes. Proc Natl Acad Sci U S A 2003;100:14199–14204.
54 Sinn PL, Sauter SL, McCray PB Jr: Gene therapy progress and prospects: development of improved lentiviral and retroviral vectors – design, biosafety, and production. Gene Ther 2005;12:1089–1098.
55 White SM, Renda M, Nam NY, Klimatcheva E, Zhu Y, Fisk J, Halterman M, Rimel BJ, Federoff H, Pandya S, Rosenblatt JD, Planelles V: Lentivirus vectors using human and simian immunodeficiency virus elements. J Virol 1999;73:2832–2840.
56 Hanawa H, Hematti P, Keyvanfar K, Metzger ME, Krouse A, Donahue RE, Kepes S, Gray J, Dunbar CE, Persons DA, Nienhuis AW: Efficient gene transfer into rhesus repopulating hematopoietic stem cells using a simian immunodeficiency virus-based lentiviral vector system. Blood 2004;103: 4062–4069.
57 Nienhuis AW, Dunbar CE, Sorrentino BP: Genotoxicity of retroviral integration in hematopoietic cells. Mol Ther 2006;13:1031–1049.
58 Kohn DB, Sadelain M, Glorioso JC: Occurrence of leukaemia following gene therapy of X-linked SCID. Nat Rev Cancer 2003;3:477–488.
59 Aiuti A, Ficara F, Cattaneo F, Bordignon C, Roncarolo MG: Gene therapy for adenosine deaminase deficiency. Curr Opin Allergy Clin Immunol 2003; 3:461–466.
60 Du Y, Jenkins NA, Copeland NG: Insertional mutagenesis identifies genes that promote the immortalization of primary bone marrow progenitor cells. Blood 2005;106:3932–3939.
61 Ott MG, Schmidt M, Schwarzwaelder K, Stein S, Siler U, Koehl U, Glimm H, Kuhlcke K, Schilz A, Kunkel H, Naundorf S, Brinkmann A, Deichmann A, Fischer M, Ball C, Pilz I, Dunbar C, Du Y, Jenkins NA, Copeland NG, Luthi U, Hassan M, Thrasher AJ, Hoelzer D, von Kalle C, Seger R, Grez M: Correction of X-linked chronic granulomatous disease by gene therapy, augmented by insertional activation of MDS1-EVI1, PRDM16 or SETBP1. Nat Med 2006;12:401–409.
62 Scherdin U, Rhodes K, Breindl M: Transcriptionally active genome regions are preferred targets for retrovirus integration. J Virol 1990;64:907–912.
63 Wu X, Li Y, Crise B, Burgess SM: Transcription start regions in the human genome are favored targets for MLV integration. Science 2003;300: 1749–1751.
64 Cavazzana-Calvo M, Hacein-Bey S, de Saint Basile G, Gross F, Yvon E, Nusbaum P, Selz F, Hue C, Certain S, Casanova JL, Bousso P, Deist FL, Fischer A: Gene therapy of human severe combined immunodeficiency (SCID)-X1 disease. Science 2000; 288:669–672.
65 Emery DW, Yannaki E, Tubb J, Nishino T, Li Q, Stamatoyannopoulos G: Development of virus vectors for gene therapy of beta chain hemoglobinopathies: flanking with a chromatin insulator reduces gamma-globin gene silencing in vivo. Blood 2002;100:2012–2019.
66 Ramezani A, Hawley TS, Hawley RG: Performance-and safety-enhanced lentiviral vectors containing the human interferon-beta scaffold attachment region and the chicken beta-globin insulator. Blood 2003;101:4717–4724.
67 West AG, Gaszner M, Felsenfeld G: Insulators: many functions, many mechanisms. Genes Dev 2002;16:271–288.
68 Gaszner M, Felsenfeld G: Insulators: exploiting transcriptional and epigenetic mechanisms. Nat Rev Genet 2006;7:703–713.

69 Yao S, Osborne CS, Bharadwaj RR, Pasceri P, Sukonnik T, Pannell D, Recillas-Targa F, West AG, Ellis J: Retrovirus silencer blocking by the cHS4 insulator is CTCF independent. Nucleic Acids Res 2003;31:5317–5323.
70 Yanez-Munoz RJ, Balaggan KS, MacNeil A, Howe SJ, Schmidt M, Smith AJ, Buch P, MacLaren RE, Anderson PN, Barker SE, Duran Y, Bartholomae C, von Kalle C, Heckenlively JR, Kinnon C, Ali RR, Thrasher AJ: Effective gene therapy with non-integrating lentiviral vectors. Nat Med 2006;12: 348–353.
71 Engelman A: In vivo analysis of retroviral integrase structure and function. Adv Virus Res 1999;52: 411–426.
72 Pierson TC, Kieffer TL, Ruff CT, Buck C, Gange SJ, Siliciano RF: Intrinsic stability of episomal circles formed during human immunodeficiency virus type 1 replication. J Virol 2002;76:4138–4144.
73 Ohmori T, Mimuro J, Takano K, Madoiwa S, Kashiwakura Y, Ishiwata A, Niimura M, Mitomo K, Tabata T, Hasegawa M, Ozawa K, Sakata Y: Efficient expression of a transgene in platelets using simian immunodeficiency virus-based vector harboring glycoprotein Ibalpha promoter: in vivo model for platelet-targeting gene therapy. FASEB J 2006;20:1522–1524.
74 Wahlers A, Schwieger M, Li Z, Meier-Tackmann D, Lindemann C, Eckert HG, von Laer D, Baum C: Influence of multiplicity of infection and protein stability on retroviral vector-mediated gene expression in hematopoietic cells. Gene Ther 2001;8: 477–486.
75 Wilcox DA, Olsen JC, Ishizawa L, Griffith M, White GC, 2nd: Integrin alphaIIb promoter-targeted expression of gene products in megakaryocytes derived from retrovirus-transduced human hematopoietic cells. Proc Natl Acad Sci U S A 1999;96: 9654–9659.
76 Schulze H, Shivdasani RA: Mechanisms of thrombopoiesis. J Thromb Haemost 2005;3:1717–1724.
77 Lepage A, Leboeuf M, Cazenave JP, de la Salle C, Lanza F, Uzan G: The alpha(IIb)beta(3) integrin and GPIb-V-IX complex identify distinct stages in the maturation of CD34(+) cord blood cells to megakaryocytes. Blood 2000;96:4169–4177.
78 Tropel P, Roullot V, Vernet M, Poujol C, Pointu H, Nurden P, Marguerie G, Tronik-Le Roux D: A 2.7-kb portion of the 5' flanking region of the murine glycoprotein alphaIIb gene is transcriptionally active in primitive hematopoietic progenitor cells. Blood 1997;90:2995–3004.
79 Nurden AT: Qualitative disorders of platelets and megakaryocytes. J Thromb Haemost 2005;3:1773–1782.
80 Tomiyama Y: Glanzmann thrombasthenia: integrin alpha IIb beta 3 deficiency. Int J Hematol 2000;72: 448–454.
81 Wilcox DA, Olsen JC, Ishizawa L, Bray PF, French DL, Steeber DA, Bell WR, Griffith M, White GC Jr: Megakaryocyte-targeted synthesis of the integrin beta(3)-subunit results in the phenotypic correction of Glanzmann thrombasthenia. Blood 2000; 95:3645–3651.
82 Fang J, Hodivala-Dilke K, Johnson BD, Du LM, Hynes RO, White GC JR, Wilcox DA: Therapeutic expression of the platelet-specific integrin, alphaI-Ibbeta3, in a murine model for Glanzmann thrombasthenia. Blood 2005;106:2671–2679.
83 Shi Q, Wilcox DA, Morateck PA, Fahs SA, Kenny D, Montgomery RR: Targeting platelet GPIbalpha transgene expression to human megakaryocytes and forming a complete complex with endogenous GPIbbeta and GPIX. J Thromb Haemost 2004;2: 1989–1997.
84 Hoyer LW: Hemophilia A. N Engl J Med 1994;330: 38–47.
85 Lozier JN, Brinkhous KM: Gene therapy and the hemophilias. JAMA 1994;271:47–51.
86 High K: Gene transfer for hemophilia: can therapeutic efficacy in large animals be safely translated to patients? J Thromb Haemost 2005;3:1682–1691.
87 Ishiwata A, Mimuro J, Kashiwakura Y, Niimura M, Takano K, Ohmori T, Madoiwa S, Mizukami H, Okada T, Naka H, Yoshioka A, Ozawa K, Sakata Y: Phenotype correction of hemophilia A mice with adeno-associated virus vectors carrying the B domain-deleted canine factor VIII gene. Thromb Res 2006;118:627–635.
88 High KA: Theodore E. Woodward Award. AAV-mediated gene transfer for hemophilia. Trans Am Clin Climatol Assoc 2003;114:337–351;discussion 351–332.
89 Kikuchi J, Mimuro J, Ogata K, Tabata T, Ueda Y, Ishiwata A, Kimura K, Takano K, Madoiwa S, Mizukami H, Hanazono Y, Kume A, Hasegawa M, Ozawa K, Sakata Y: Sustained transgene expression by human cord blood derived CD34+ cells transduced with simian immunodeficiency virus agmTYO1-based vectors carrying the human coagulation factor VIII gene in NOD/SCID mice. J Gene Med 2004;6:1049–1060.
90 Kootstra NA, Matsumura R, Verma IM: Efficient production of human FVIII in hemophilic mice using lentiviral vectors. Mol Ther 2003;7:623–631.
91 Wilcox DA, Shi Q, Nurden P, Haberichter SL, Rosenberg JB, Johnson BD, Nurden AT, White GC Jr, Montgomery RR: Induction of megakaryocytes to synthesize and store a releasable pool of human factor VIII. J Thromb Haemost 2003;1:2477–2489.
92 Shi Q, Wilcox DA, Fahs SA, Fang J, Johnson BD, Du LM, Desai D, Montgomery RR: Lentivirus-mediated platelet-derived factor VIII gene therapy in murine haemophilia A. J Thromb Haemost 2007;5: 352–361.
93 Chang AH, Stephan MT, Sadelain M: Stem cell-derived erythroid cells mediate long-term systemic protein delivery. Nat Biotechnol 2006;24:1017–1021.
94 Kohn DB: Lentiviral vectors ready for prime-time. Nat Biotechnol 2007;25:65–66.

Silencing of a Targeted Protein in In Vivo Platelets Using a Lentiviral Vector Delivering Short Hairpin RNA Sequence

Tsukasa Ohmori, Yuji Kashiwakura, Akira Ishiwata, Seiji Madoiwa, Jun Mimuro, Yoichi Sakata

Objective—Because platelets are anucleate cells having a limited life span, direct gene manipulation cannot in principle be used to investigate the involvement of a specific signal transduction pathway in platelet activation. In this study, we examined whether the expression of a short hairpin RNA (shRNA) sequence in hematopoietic stem cells is maintained during megakaryocyte differentiation, thus resulting in inhibition of targeted protein in platelets.

Methods and Results—To identify platelets derived from transduced stem cells, we generated a lentiviral vector that simultaneously expresses the shRNA sequence driven by the U6 promoter and GFP under the control of the glycoprotein (GP) Ibα promoter. Transplantation of mouse bone marrow cells transduced with the vector facilitated specifically mark platelets derived from the transduced cells. Transplantation of cells transduced with shRNA sequence targeting integrin αIIb caused a significant reduction of integrin αIIbβ3 (αIIbβ3) expression in GFP-positive platelets. It also inhibited αIIbβ3 activation assessed by the binding of JON/A, an antibody that recognizes activated αIIbβ3. Talin-1 silencing by the same method resulted in normal αIIbβ3 expression but deficient inside-out αIIbβ3 signaling.

Conclusions—shRNA expression driven by the U6 promoter is preserved during megakaryopoiesis. This method facilitates functional analysis of targeted protein in platelet activation. ***(Arterioscler Thromb Vasc Biol. 2007;27:2266-2272.)***

Key Words: shRNA ■ RNA interference ■ platelets ■ talin ■ integrin

Platelets are terminally-differentiated circulating anucleate cells whose adhesive and signaling functions are essential for normal hemostasis. Platelets are produced in the bone marrow from megakaryocytes as cytoplasmic fragments without genomic DNA.[1] Although platelets contain mRNA within their cytoplasm and can respond to physiological stimuli using biosynthetic processes regulated at the protein translation level,[2,3] application of direct genetic manipulation in platelets has not been reported. Alternatively, megakaryocyte lineage cells derived from embryonic or hematopoietic stem cells are amenable to genetic manipulation using gene transduction systems, enabling molecular studies of adhesion and signaling in megakaryocytes in a way not possible with platelets.[4,5]

Because platelets and their precursor megakaryocytes have a finite lifespan, hematopoietic stem cells are preferable targets for genetic transfer to establish long-term in vivo expression of the targeted protein in platelets.[6] When a retroviral vector containing the integrin β3 (β3) gene driven by the integrin αIIb (αIIb) promoter was transduced into $CD34^+$ cells from a Glanzmann thrombasthenia patient with defects in the β3 gene, integrin αIIbβ3 (αIIbβ3) was detected after in vitro megakaryocyte differentiation.[7] We have previously shown that transduction of hematopoietic stem cells with lentiviral vector harboring the glycoprotein (GP) Ibα promoter enables specific and efficient expression of the targeted protein in platelets in vivo.[8] Further, the therapeutic expression of αIIbβ3 in β3-deficient mice using a lentivirus vector containing β3 complimentary DNA (cDNA) under the control of the αIIb promoter has been reported.[9] These data indicate that gene expression driven by a platelet-specific promoter using the transduction of hematopoietic stem cells with lentiviral vector can be applied to investigations of the involvement of specific proteins in platelet signaling pathways. However, there has been no evaluation of whether the knock-down of targeted proteins in hematopoietic stem cells using a short hairpin RNA (shRNA) sequence results in sufficient protein reduction in platelets. In this study, we examined whether shRNA expression driven by the RNA polymerase III promoter is sustained during megakaryopoiesis, and whether gene silencing with shRNAs is applicable to analyzing the functions of αIIbβ3 in in vivo platelets.

Materials and Methods

Materials, cDNA cloning, transfection, construction of lentiviral vector, stem cell transplantation, flow cytometry, immunoblotting, RT-polymerase chain reaction (PCR), platelet adhesion assay, and

Original received March 26, 2007; final version accepted July 19, 2007.

From the Research Division of Cell and Molecular Medicine, Center for Molecular Medicine, Jichi Medical University School of Medicine, Tochigi, Japan.

Correspondence to Tsukasa Ohmori, MD, PhD or Yoichi Sakata, MD, PhD, Research Division of Cell and Molecular Medicine, Center for Molecular Medicine, Jichi Medical University School of Medicine, 3111-1 Yakushiji, Shimotsuke, Tochigi 329-0498, Japan. E-mail tohmori@jichi.ac.jp or yoisaka@jichi.ac.jp.

Arterioscler Thromb Vasc Biol. is available at http://atvb.ahajournals.org DOI: 10.1161/ATVBAHA.107.149872

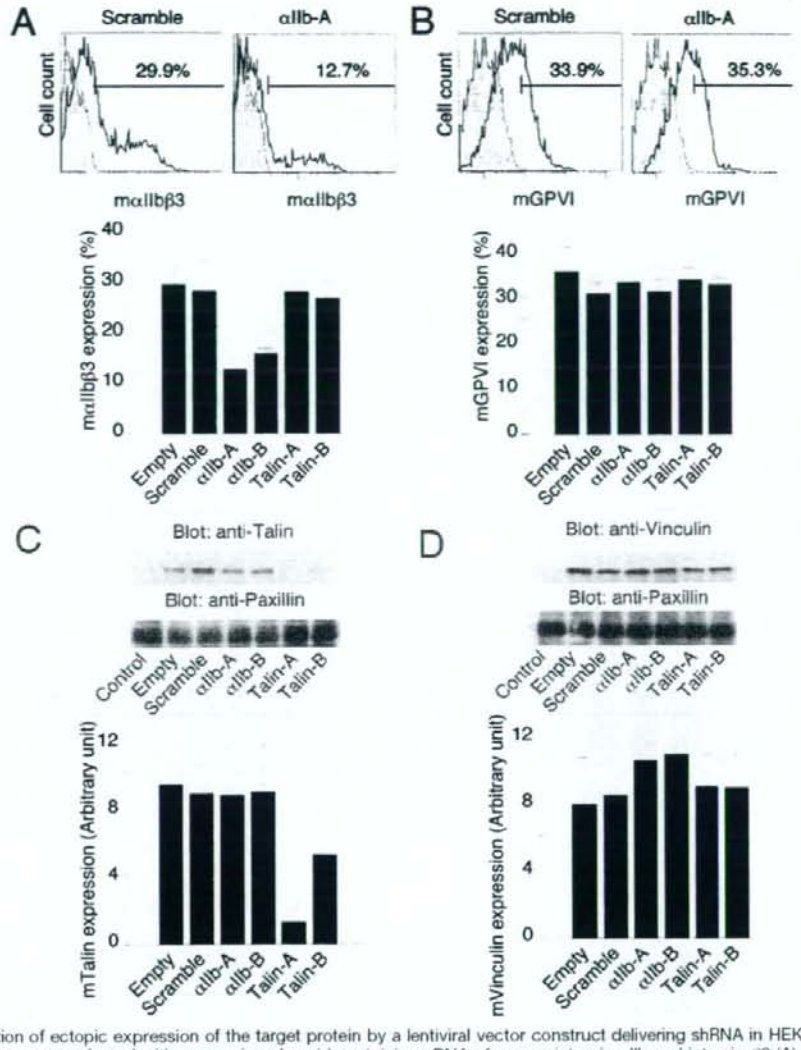

Figure 1. Inhibition of ectopic expression of the target protein by a lentiviral vector construct delivering shRNA in HEK293 cells. HEK293 cells were cotransfected with expression plasmid containing cDNA of mouse integrin αIIb and integrin β3 (A), GPVI (B), Talin (C), or vinculin (D) and the lentiviral siRNA vector plasmid containing no RNA sequence (Empty), scramble RNA sequence (Scramble), αIIbA sequence (αIIb-A), αIIbB sequence (αIIb-B), talinA sequence (Talin-A), or talinB sequence (Talin-B). After 48 hours, protein expressions were examined by flow cytometry or immunoblotting. The data are representative of 3 experiments. In lower panel, protein expression after transfection was quantified. Columns and error bars represent the mean±SD (n=3 per group).

immunohistochemistry are described in detail in the supplemental materials, available online at http://atvb.ahajournals.org.

Results

Efficient GFP Expression in Platelets Using LentiLox Vector Harboring *GPIbα* Promoter In Vivo

We first substituted the CMV promoter of pLL3.7, a lentiviral gene transfer vector which simultaneously expresses shRNA and GFP (LentiLox-CMV),[10] with the platelet-specific GPIbα promoter (LentiLox-GPIbα) (supplemental Figure I). To compare strengths and the specificities of the CMV and GPIbα promoters and to assess GFP transduction using these lentiviral vectors in vivo, bone marrow cells transduced with LentiLox-CMV or LentiLox-GPIbα were transplanted into the recipient mice. When bone marrow cells transduced with LentiLox-CMV were transplanted, GFP expression was observed in 14% to 32% of $CD45^+$ cells and in 0.7 to 2.4% of platelets in peripheral blood (supplemental Figure II). As described previously,[8] transduction with LentiLox-GPIbα resulted in efficient GFP gene marking in platelets (10% to 22%); however, only marginal GFP expression was observed in $CD45^+$ and red blood cells (supplemental Figure II). These data suggested that the LentiLox-GPIbα

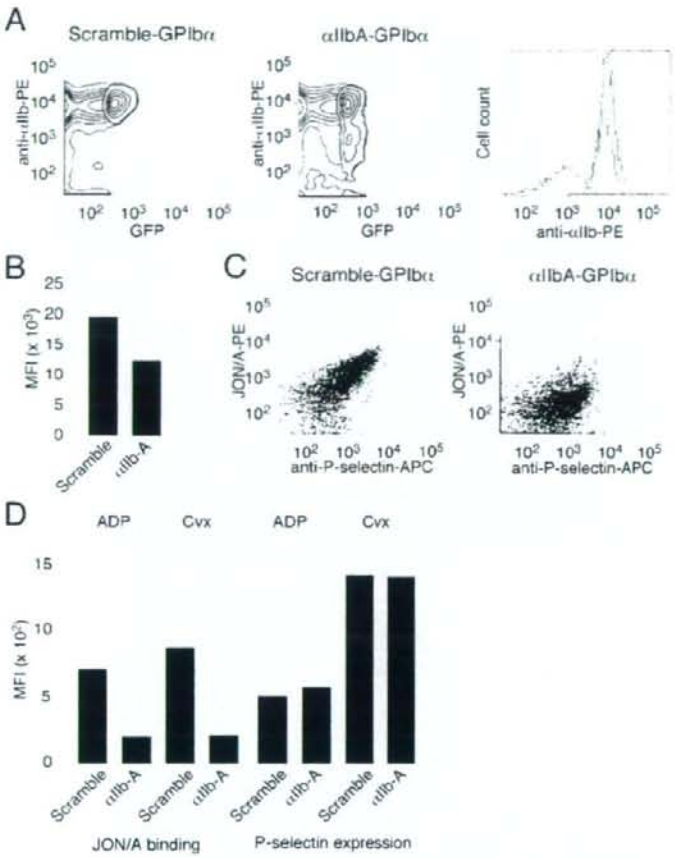

Figure 2. Silencing of endogenous integrin $\alpha IIb\beta 3$ in platelets. Bone marrow cells from donor mice were transduced with LentiLox-scramble-GPIbα or LentiLox-αIIbA-GPIbα at an MOI of 30. Each irradiated recipient mouse received 2 000 000 transduced cells. A, Representative flow cytometry analyses of integrin $\alpha IIb\beta 3$ expression in platelets of peripheral blood are shown 30 days after transplantation. The plots represent the degree of GFP expression (horizontal) and specific antibody binding for integrin αIIb (vertical). The specific antibody binding in GFP-positive platelets is shown (right panel; white:Lentilox-scramble-GPIbα, gray: LentiLox-αIIbA-GPIbα). B, Columns and error bars represent the mean ± SD of mean fluorescence intensity of antibody binding for αIIb in GFP-positive platelets (n = 9 per group). C, The activation of $\alpha IIb\beta 3$ assessed by JON/A binding and P-selectin expression in platelets stimulated with 150 ng/mL of convulxin. The plots represent the degree of P-selectin expression (horizontal) and JON/A binding (vertical) in GFP-positive platelets. D, Columns and error bars represent the mean ± SD of mean fluorescence intensity (MFI) of antibody binding after stimulation with 6 μmol/L ADP or 150 ng/mL of convulxin to GFP-positive platelets (n = 5 to 7 per group).

system enables specific GFP marking of platelets derived from transduced hematopoietic stem cells.

Efficiency of Lentiviral shRNA for Silencing of Targeted Protein Expression

We next validated the effects of shRNA sequence expression driven by the U6 promoter in LentiLox on expression of the targeted protein. We selected the shRNA sequences for integrin αIIb (supplemental Figure IB), so that it was easy to validate the expression and function of this protein using flow cytometry. We also chose talin-1 sequences as a test case for intracellular protein (supplemental Figure IB); because talin is responsible for β integrin activation but its function in in vivo platelets has not been evaluated. Because a molecular defect affecting 1 of the 2 integrin-coding genes is sufficient to cause a concomitant deficit of both αIIb and β3,[11] we prepared the 2 expression plasmids containing cDNA of αIIb and β3 for the expression of $\alpha IIb\beta 3$ complexes. To determine the efficiency of lentiviral shRNA for αIIb-A, the surface expression of $\alpha IIb\beta 3$ in HEK293 cells was determined after cotransfection of the shRNA constructs with integrin αIIb and β3 expression plasmids. As shown in Figure 1A, $\alpha IIb\beta 3$ expression on the cell surface was significantly inhibited by cotransfection with the shRNA constructs for αIIb. On the other hand, other shRNA sequences did not affect the surface expression of $\alpha IIb\beta 3$ (Figure 1A). As well, shRNA sequences for talin-1 specifically inhibited ectopically-expressed talin in HEK293 cells (Figure 1C). Sequences for αIIb-A and talin did not influence the expressions of GPVI and vinculin (Figure 1B and 1D). The degradation of mRNA by shRNA expression was confirmed by real-time quantitative RT-PCR (supplemental Figure III). The construct expressing the shRNA sequence αIIb-A and talin-A caused a more powerful inhibition of the expressions of αIIb and talin, respectively (Figure 1A and 1C). To rule out the off-targeting effect caused by the high concentration of shRNA, we validated the specificity of these shRNA sequences by a lower concentration of plasmid vectors (0.2 μg; data not shown). Hence, we selected the αIIbA and talin-A sequences for in vivo experiments.

Silencing of $\alpha IIb\beta 3$ Expression In Vivo Platelets by Transplantation of Transduced Bone Marrow Cells With shRNA Lentiviral Vector

We next examined the effects of shRNA driven by the U6 promoter during megakaryopoiesis in vivo. The bone marrow cells transduced with LentiLox-GPIb containing the scramble

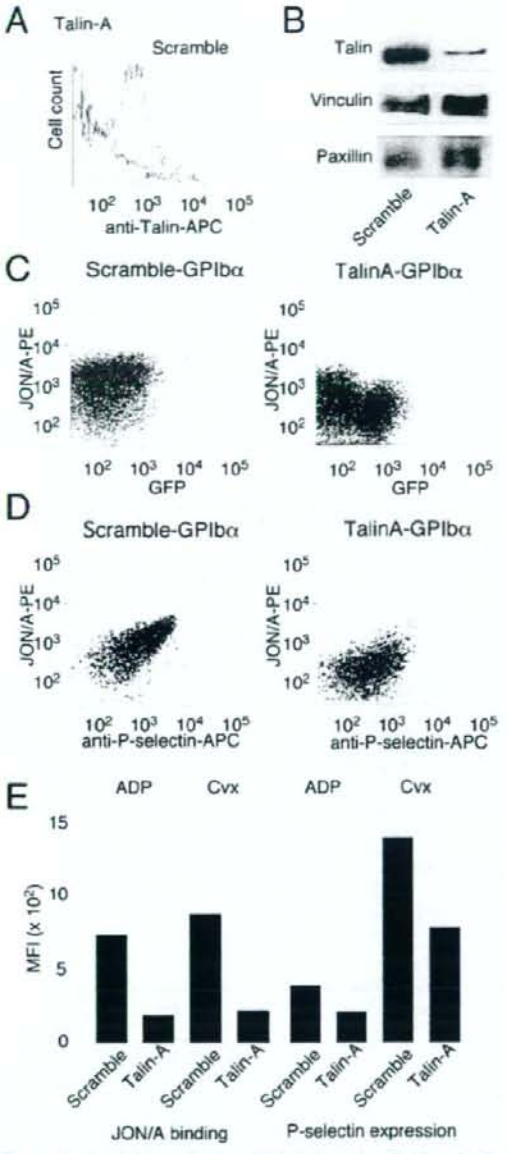

Figure 3. Knockdown of talin-1 inhibits integrin αIIbβ3 activation and P-selectin expression in platelets. Bone marrow cells transfected with LentiLox-scramble-GPIbα or LentiLox-talinA-GPIbα were transplanted into recipient mice. A, Representative flowcytometry analyses of intracellular talin expression in GFP-positive (white: LentiLox-scramble-GPIbα; gray: Lentilox-talinA-GPIbα). B, After the sorting of GFP-positive platelets, the platelet lysates were immunoblotted with anti-talin MoAb (upper panel), anti-vinculin polyclonal antibody (middle panel), or anti-paxillin antibody (lower panel). C, Activation of αIIbβ3 was assessed by JON/A binding to platelets incubated with 150 ng/mL of convulxin. The plots represent the degree of GFP expression (horizontal) and specific antibody binding (vertical). D, Activation of αIIbβ3 assessed by JON/A binding and P-selectin expression in GFP-positive platelets stimulated with 150 ng/mL of convulxin. The plots represent the degree of P-selectin expression (horizontal) and JON/A binding (vertical). E, Columns and error bars represent the mean ± SD of mean fluorescence intensity (MFI) of antibody binding after stimulation with 6 μmol/L ADP or 150 ng/mL of convulxin to GFP-positive platelets (n = 7 to 11 per group).

sequence (LentiLox-scramble-GPIbα) or αIIbA sequence (LentiLox-αIIbA-GPIbα) were transplanted into recipient mice. After transplantation, GFP expression was observed in 15% to 20% of platelets in both transplanted groups (data not shown). It is of note that αIIbβ3 expression in GFP-positive platelets was significantly reduced in the recipient mice transplanted with cells transduced with LentiLox-αIIbA-GPIbα (Figure 2A and 2B). As well, JON/A binding after ADP stimulation, which recognizes activated αIIbβ3, was reduced to a greater extent by the transduction with LentiLox-αIIbA-GPIbα (Figure 2B and 2D). The discrepancy in the results between αIIbβ3 expression and JON/A binding is thought to be partly the result of the expression of an incompetent αIIbβ3 complex that is recognized as antigen but does not act as functional receptor. Because αIIb is the most abundant protein in platelets, it is possible that mRNA degradation of αIIb by siRNA in platelets becomes incomplete. Under the same conditions, GPIb and GPVI expressions were not affected (data not shown). Additionally, P-selectin expression after platelet activation was hardly affected (Figure 2C and 2D). These data suggested that the expression of the shRNA sequence driven by the U6 promoter is maintained during megakaryopoiesis, and that this method can be applied to investigations of the involvement of specific proteins in platelet activation.

Silencing of Talin in Platelets Decreases αIIbβ3 Activation

We next examined whether talin-1 knockdown affects αIIbβ3 activation in in vivo platelets, using shRNA silencing. Although talin is believed to be involved in the final common step of integrin αIIbβ3 activation,[12] functional analysis in in vivo platelets has not been performed. When bone marrow cells transduced with LentiLox-scramble-GPIbα or LentiLox-talinA-GPIbα at an MOI of 30 were transplanted, we confirmed the inhibition of talin expression in platelets derived from the cells transduced with LentiLox-talinA-GPIbα by intracellular flowcytometry (Figure 3A). In addition, talin reduction was also verified after sorting of GFP-positive platelets by immunoblotting (Figure 3B). On the other hand, the expressions of αIIbβ3, GPIbα, and GPVI were not affected (data not shown). As shown in Figure 3C through 3E, in talin-deficient platelets identified as GFP-positive cells, αIIbβ3 activation after ADP or convulxin stimulation was significantly decreased. Furthermore, talin-deficient platelet partly affected the expression of P-selectin after the platelet stimulation (Figure 3D and 3E). These data clarified that talin was involved not only in αIIbβ3-dependent platelet activation but also in the release reaction in actual platelets.

Finally, using a platelet adhesion assay we attempted to determine whether talin-deficient platelets influenced the spreading onto fibrinogen. Platelet adhesion to immobilized

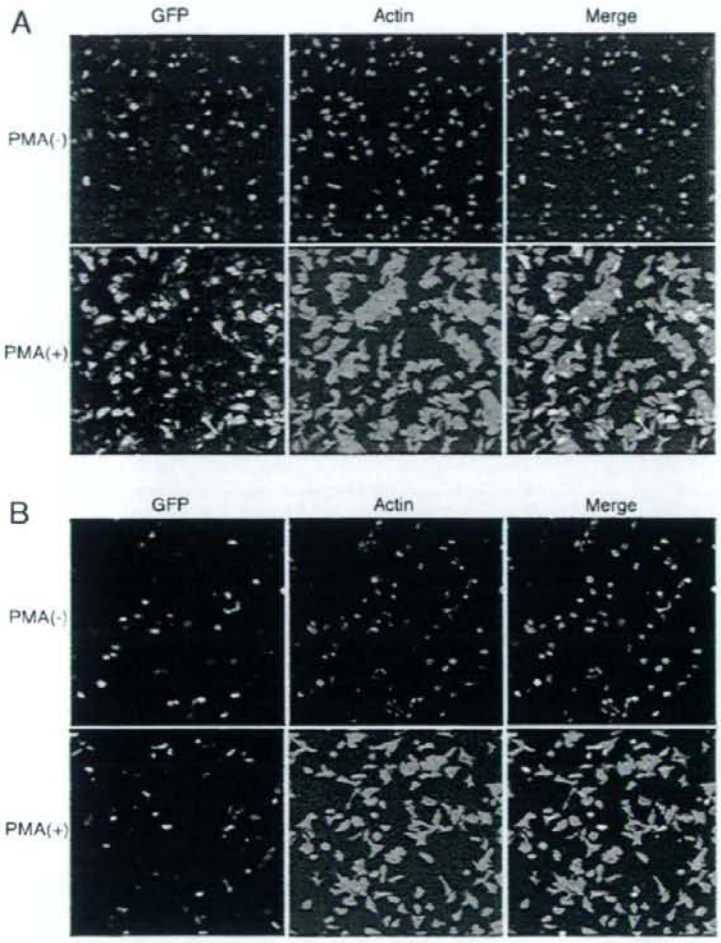

Figure 4. Failure of talin-deficient platelets to spread onto immobilized fibrinogen after stimulation with PMA. Bone marrow cells transfected with LentiLox-scramble-GPIbα (A) or LentiLox-talinA-GPIbα (B) were transplanted into recipient mice. Washed platelets treated without (upper panel) or with 1 μmol/L PMA (lower panel) were placed on immobilized fibrinogen for 30 minutes. Cells were fixed and then stained with anti-GFP antibody (green; left panel) and rhodamine-conjugated phalloidin (red; middle panel), as described in Materials and Methods. The merged images show colocalization of GFP and actin staining (yellow; right panel). The data are representative of 3 independent experiments.

fibrinogen by itself was not inhibited by the deficiency of talin (Figure 4). However, platelet spreading after stimulation with PMA was markedly suppressed (Figure 4), suggesting that talin is required for platelet spreading on fibrinogen.

Discussion

RNA interference using siRNAs to inhibit specific gene expression is a powerful and promising technology for both basic research and therapeutic intervention.[13,14] A number of vector systems have been reported to mediate stable transduction and expression of shRNAs in mammalian cells.[13] Among them, lentiviral vectors have been demonstrated to have the ability to stably transduce nondividing cells such as stem cells through integration of the vector DNA into the genome.[10,15] RNA polymerase III promoters, most commonly the H1 and U6 promoters, have been incorporated into the lentiviral vectors for stable expression of shRNAs.[13] The potential problem for functional genomics studies inherent in transfection with shRNA is variability in transfection efficiency. A solution to this problem is coexpression of reporter genes such as GFP, which facilitates the selection of transduced cells. To obtain efficient gene marking of platelets derived from transduced hematopoietic stem cells, we substituted the ubiquitous CMV promoter of LentiLox with the platelet-specific GPIbα promoter and showed that transplantation of bone marrow cells transduced with the vector enabled specific marking of platelets derived from transduced hematopoietic stem cells expressing shRNA sequence.

Platelets are terminally-differentiated anucleate cells, and for this reason direct gene transfer and silencing using virus or plasmid vector have been thought to be impossible. Since the development of gene targeting technologies in embryonic stem cells,[16] the "gold standard" for the analysis of gene function in platelets has been the creation of knockout mice. A large number of knockout studies have shown aberrant platelet phenotypes.[17–20] However, one of the major drawbacks of conventional knockouts is that if the gene product is essential in many tissues, then it is quite likely that the consequence of homozygosity for the mutated allele will be lethality. Several experimental strategies are used or have the

potential to overcome the problem of lethality. First, improvements in the technological procedures have allowed for refined analyses of gene functions at specific developmental stages or in specific tissues, based on conditional knock-out strategies by means of Cre-lox–regulated recombination.[21] Another solution, which has been applied in a few cases, is to use hematopoietic cells from fetal liver of knockout embryos to reconstitute the hematopoietic system of lethally-irradiated wild-type animals.[22,23] Despite these significant improvements, the creation of loss-of-function alleles in the mouse remains time-consuming and costly. Our demonstration that the expression of shRNAs driven by RNA polymerase III promoters can be used to functionally silence protein expression in platelets suggests that RNAi-based technologies might represent a convenient strategy for the study of platelet signal transduction. Our methods could in fact detect platelets derived from transduced stem cells as GFP-positive platelets, and so enable the examination of the involvement of target proteins in platelet signal transduction by flow cytometry and adhesion assay. However, GFP-positive platelets after the transplantation were limited by up to 20% in our protocols. Hence, platelet aggregation testing and the analysis of intracellular signaling pathways including tyrosine phosphorylation are not thought impossible. Higher transfection efficiencies would be required to demonstrate genuine effects and to be a valid alternative to making gene knockout mice.

Cellular control of integrin activation is essential for normal development because it controls cell adhesion, migration, and assembly of the extracellular matrix.[24,25] Platelets express members of the $\beta 1$ subfamily ($\alpha v\beta 1$, $\alpha 2\beta 1$, and $\alpha 6\beta 1$) that support platelet adhesion to the extracellular matrix proteins including collagen and laminins, as well as expressing members of the $\beta 3$ subfamily ($\alpha v\beta 3$ and $\alpha IIb\beta 3$).[24] Among them, $\alpha IIb\beta 3$, a receptor for fibrinogen, von Willebrand factor (VWF), fibronectin, and vitronectin is an essential requirement for platelet aggregation. Integrin activation can be controlled by signaling pathways that are thought to act by regulating specific interactions between cytoplasmic proteins and the integrin—or β-subunit—cytoplasmic tail.[25,26] Although many types of proteins interacting with integrin cytoplasmic tails have been reported to be involved in platelet aggregation,[12,27–31] functional analysis of in vivo platelets has not been reported; embryos lacking these proteins, including talin, vinculin, FAK, and Cas do not normally grow in the uterus.[32–35] Talin is a major cytoskeletal protein that colocalizes with activated integrins and binds to integrin β cytoplasmic domains; with the overexpression of the N-terminal region of talin results in activation of integrins.[14,28,36] Additionally, binding of talin to integrin β tails has been shown to be a common final step in integrin activation.[12] In this study, using a method involving RNA interference, we clearly demonstrated that talin is involved in $\alpha IIb\beta 3$-dependent platelet activation in in vivo platelets. Furthermore, talin might partly participate in the α-granule release reaction. These results confirmed that this strategy could be useful as a convenient and powerful method to investigate the role of specific proteins in platelet activation in vivo.

Acknowledgments

We thank N. Matsumoto and M. Ito for their excellent technical assistance.

Sources of Funding

This work was supported by Grants from the Mitsubishi Pharma Research Foundation; Grants-in-aid for Scientific Research from the Ministry of Education and Science; Health and Labor Science Research Grants for Research from Ministry of Health, Labor, and Welfare; and Grants for "High-Tech Center Research" Projects for Private Universities: matching fund subsidy from MEXT (Ministry of Education, Culture, Sports, Science, and Technology), 2002–2006.

Disclosures

None.

References

1. Italiano JE Jr, Shivdasani RA. Megakaryocytes and beyond: the birth of platelets. *J Thromb Haemost*. 2003;1:1174–1182.
2. Brogren H, Karlsson L, Andersson M, Wang L, Erlinge D, Jern S. Platelets synthesize large amounts of active plasminogen activator inhibitor 1. *Blood*. 2004;104:3943–3948.
3. Maguire PB, Fitzgerald DJ. Platelet proteomics. *J Thromb Haemost*. 2003;1:1593–1601.
4. Eto K, Murphy R, Kerrigan SW, Bertoni A, Stuhlmann H, Nakano T, Leavitt AD, Shattil SJ. Megakaryocytes derived from embryonic stem cells implicate CalDAG-GEFI in integrin signaling. *Proc Natl Acad Sci U S A*. 2002;99:12819–12824.
5. Shiraga M, Ritchie A, Aidoudi S, Baron V, Wilcox D, White G, Ybarrondo B, Murphy G, Leavitt A, Shattil S. Primary megakaryocytes reveal a role for transcription factor NF-E2 in integrin alpha IIb beta 3 signaling. *J Cell Biol*. 1999;147:1419–1430.
6. Wilcox DA, White GC 2nd. Gene therapy for platelet disorders: studies with Glanzmann's thrombasthenia. *J Thromb Haemost*. 2003;1:2300–2311.
7. Wilcox DA, Olsen JC, Ishizawa L, Bray PF, French DL, Steeber DA, Bell WR, Griffith M, White GC 2nd. Megakaryocyte-targeted synthesis of the integrin beta(3)-subunit results in the phenotypic correction of Glanzmann thrombasthenia. *Blood*. 2000;95:3645–3651.
8. Ohmori T, Mimuro J, Takano K, Madoiwa S, Kashiwakura Y, Ishiwata A, Niimura M, Mitomo K, Tabata T, Hasegawa M, Ozawa K, Sakata Y. Efficient expression of a transgene in platelets using simian immunodeficiency virus-based vector harboring glycoprotein Ibalpha promoter: in vivo model for platelet-targeting gene therapy. *Faseb J*. 2006;20:1522–1524.
9. Fang J, Hodivala-Dilke K, Johnson BD, Du LM, Hynes RO, White GC 2nd, Wilcox DA. Therapeutic expression of the platelet-specific integrin, alphaIIbbeta3, in a murine model for Glanzmann thrombasthenia. *Blood*. 2005;106:2671–2679.
10. Rubinson DA, Dillon CP, Kwiatkowski AV, Sievers C, Yang L, Kopinja J, Rooney DL, Ihrig MM, McManus MT, Gertler FB, Scott ML, Van Parijs L. A lentivirus-based system to functionally silence genes in primary mammalian cells, stem cells and transgenic mice by RNA interference. *Nat Genet*. 2003;33:401–406.
11. Perutelli P, Mori PG. Biochemical and molecular basis of Glanzmann's thrombasthenia. *Haematologica*. 1992;77:421–426.
12. Tadokoro S, Shattil SJ, Eto K, Tai V, Liddington RC, de Pereda JM, Ginsberg MH, Calderwood DA. Talin binding to integrin beta tails: a final common step in integrin activation. *Science*. 2003;302:103–106.
13. Amarzguioui M, Rossi JJ, Kim D. Approaches for chemically synthesized siRNA and vector-mediated RNAi. *FEBS Lett*. 2005;579:5974–5981.
14. Li CX, Parker A, Menocal E, Xiang S, Borodyansky L, Fruehauf JH. Delivery of RNA interference. *Cell Cycle*. 2006;5:2103–2109.
15. Woods NB, Ooka A, Karlsson S. Development of gene therapy for hematopoietic stem cells using lentiviral vectors. *Leukemia*. 2002;16:563–569.
16. Thomas KR, Capecchi MR. Site-directed mutagenesis by gene targeting in mouse embryo-derived stem cells. *Cell*. 1987;51:503–512.
17. Clements JL, Lee JR, Gross B, Yang B, Olson JD, Sandra A, Watson SP, Lentz SR, Koretzky GA. Fetal hemorrhage and platelet dysfunction in SLP-76-deficient mice. *J Clin Invest*. 1999;103:19–25.

18. Pasquet JM, Gross B, Quek L, Asazuma N, Zhang W, Sommers CL, Schweighoffer E, Tybulewicz V, Judd B, Lee JR, Koretzky G, Love PE, Samelson LE, Watson SP. LAT is required for tyrosine phosphorylation of phospholipase cgamma2 and platelet activation by the collagen receptor GPVI. *Mol Cell Biol.* 1999;19:8326–8334.
19. Watson SP, Gibbins J. Collagen receptor signalling in platelets: extending the role of the ITAM. *Immunol Today.* 1998;19:260–264.
20. Offermanns S. Activation of platelet function through G protein-coupled receptors. *Circ Res.* 2006;99:1293–1304.
21. Tiedt R, Schomber T, Hao-Shen H, Skoda RC. Pf4-Cre transgenic mice allow generating lineage-restricted gene knockouts for studying megakaryocyte and platelet function in vivo. *Blood.* 2006.
22. Obergfell A, Eto K, Mocsai A, Buensuceso C, Moores SL, Brugge JS, Lowell CA, Shattil SJ. Coordinate interactions of Csk, Src, and Syk kinases with αIIbβ3 initiate integrin signaling to the cytoskeleton. *J Cell Biol.* 2002;157:265–275.
23. Matloubian M, Lo CG, Cinamon G, Lesneski MJ, Xu Y, Brinkmann V, Allende ML, Proia RL, Cyster JG. Lymphocyte egress from thymus and peripheral lymphoid organs is dependent on S1P receptor 1. *Nature.* 2004;427:355–360.
24. Bennett JS. Structure and function of the platelet integrin alphaIIbbeta3. *J Clin Invest.* 2005;115:3363–3369.
25. Zamir E, Geiger B. Molecular complexity and dynamics of cell-matrix adhesions. *J Cell Sci.* 2001;114:3583–3590.
26. Lo SH. Focal adhesions: what's new inside. *Dev Biol.* 2006;294:280–291.
27. Asijee GM, Sturk A, Bruin T, Wilkinson JM, Ten Cate JW. Vinculin is a permanent component of the membrane skeleton and is incorporated into the (re)organising cytoskeleton upon platelet activation. *Eur J Biochem.* 1990;189:131–136.
28. Calderwood DA, Zent R, Grant R, Rees DJ, Hynes RO, Ginsberg MH. The Talin head domain binds to integrin beta subunit cytoplasmic tails and regulates integrin activation. *J Biol Chem.* 1999;274:28071–28074.
29. Lipfert L, Haimovich B, Schaller MD, Cobb BS, Parsons JT, Brugge JS. Integrin-dependent phosphorylation and activation of the protein tyrosine kinase pp125FAK in platelets. *J Cell Biol.* 1992;119:905–912.
30. Ohmori T, Yatomi Y, Asazuma N, Satoh K, Ozaki Y. Involvement of proline-rich tyrosine kinase 2 in platelet activation: tyrosine phosphorylation mostly dependent on alphaIIbbeta3 integrin and protein kinase C, translocation to the cytoskeleton and association with Shc through Grb2. *Biochem J.* 2000;347:561–569.
31. Ohmori T, Yatomi Y, Inoue K, Satoh K, Ozaki Y. Tyrosine dephosphorylation, but not phosphorylation, of p130Cas is dependent on integrin alpha IIb beta 3-mediated aggregation in platelets: implication of p130Cas involvement in pathways unrelated to cytoskeletal reorganization. *Biochemistry.* 2000;39:5797–5807.
32. Honda H, Oda H, Nakamoto T, Honda Z, Sakai R, Suzuki T, Saito T, Nakamura K, Nakao K, Ishikawa T, Katsuki M, Yazaki Y, Hirai H. Cardiovascular anomaly, impaired actin bundling and resistance to Src-induced transformation in mice lacking p130Cas. *Nat Genet.* 1998;19:361–365.
33. Ilic D, Furuta Y, Kanazawa S, Takeda N, Sobue K, Nakatsuji N, Nomura S, Fujimoto J, Okada M, Yamamoto T. Reduced cell motility and enhanced focal adhesion contact formation in cells from FAK-deficient mice. *Nature.* 1995;377:539–544.
34. Monkley SJ, Zhou XH, Kinston SJ, Giblett SM, Hemmings L, Priddle H, Brown JE, Pritchard CA, Critchley DR, Fassler R. Disruption of the talin gene arrests mouse development at the gastrulation stage. *Dev Dyn.* 2000;219:560–574.
35. Xu W, Baribault H, Adamson ED. Vinculin knockout results in heart and brain defects during embryonic development. *Development.* 1998;125:327–337.
36. Calderwood DA. Talin controls integrin activation. *Biochem Soc Trans.* 2004;32:434–437.

Adenoassociated Virus–Mediated Prostacyclin Synthase Expression Prevents Pulmonary Arterial Hypertension in Rats

Takayuki Ito, Takashi Okada, Jun Mimuro, Hiroshi Miyashita, Ryosuke Uchibori, Masashi Urabe, Hiroaki Mizukami, Akihiro Kume, Masafumi Takahashi, Uichi Ikeda, Yoichi Sakata, Kazuyuki Shimada, Keiya Ozawa

Abstract—Prostacyclin synthase (PGIS) is the final committed enzyme in the metabolic pathway of prostacyclin production. The therapeutic option of intravenous prostacyclin infusion in patients with pulmonary arterial hypertension is limited by the short half-life of the drug and life-threatening catheter-related complications. To develop a better delivery system for prostacyclin, we examined the feasibility of intramuscular injection of an adenoassociated virus (AAV) vector expressing PGIS for preventing monocrotaline-induced pulmonary arterial hypertension in rats. We developed an AAV serotype 1–based vector carrying a human PGIS gene (AAV-PGIS). AAV-PGIS or the control AAV vector expressing enhanced green fluorescent protein was injected into the anterior tibial muscles of 3-week–old male Wistar rats; this was followed by the monocrotaline administration at 7 weeks. Eight weeks after injecting the vector, the plasma levels of 6-keto-prostaglandin $F_{1\alpha}$ increased in a vector dose-dependent manner. At this time point, the PGIS transduction (1×10^{10} genome copies per body) significantly decreased mean pulmonary arterial pressure (33.9 ± 2.4 versus 46.1 ± 3.0 mm Hg; $P<0.05$), pulmonary vascular resistance (0.26 ± 0.03 versus 0.41 ± 0.03 mm Hg $\cdot$ mL$^{-1}\cdot$ min$^{-1}\cdot$ kg^{-1}; $P<0.05$), and medial thickness of the peripheral pulmonary artery ($14.6\pm1.5\%$ versus $23.5\pm0.5\%$; $P<0.01$) as compared with the controls. Furthermore, the PGIS-transduced rats demonstrated significantly improved survival rates as compared with the controls (100% versus 50%; $P<0.05$) at 8 weeks postmonocrotaline administration. An intramuscular injection of AAV-PGIS prevents monocrotaline-pulmonary arterial hypertension in rats and provides a new therapeutic alternative for preventing pulmonary arterial hypertension in humans. (***Hypertension.*** **2007;50:531-536.)**

Key Words: hypertension ■ pulmonary ■ gene therapy ■ remodeling ■ prostacyclin synthase

Pulmonary arterial hypertension (PAH) is an intractable disease that leads to increased pulmonary arterial pressure, progressive right heart failure, and premature death; however, no satisfactory treatment has been established for PAH.[1] Although intravenous prostacyclin (PGI_2) therapy prolongs survival in patients with PAH, the use of this treatment option is limited by the short half-life of the drug, requirement for a continuous infusion system, and catheter-related complications.[1,2] PGI_2 synthase (PGIS) is the final committed enzyme in the metabolic pathway of PGI_2 production. PGIS gene transfer is a promising approach for the stable production of endogenous PGI_2.[3–6] However, previous strategies have several limitations both in the selection of delivery routes and in the efficiency of gene expression. For instance, intratracheal gene transfer may deteriorate respiratory function in critically ill subjects, and the intrahepatic approach may cause peritonitis as a result of direct liver puncture. Although an intramuscular approach seems to be safer than the previous approaches, the conventional plasmid-based strategies achieved only transient gene expression and required repeated gene transfer to inhibit pathological remodeling of the pulmonary artery (PA).[6]

In this study, we used an adenoassociated virus (AAV) vector together with an intramuscular approach to obtain more efficient PGI_2 expression. AAV vectors permit efficient and sustained gene expression in nondividing skeletal muscle cells with minimal inflammatory and immune responses. We reported previously that a stable serum concentration of a secretory protein was achieved over a 1-year period by using a single intramuscular injection of several AAV vector (AAV2 and AAV5) serotypes in mice.[7] Currently, AAV1 is one of the most efficient serotypes for muscle transduction.[8,9]

Received March 25, 2007; first decision April 13, 2007; revision accepted June 22, 2007.

From the Divisions of Genetic Therapeutics (T.I., R.U., M.U., H.M., A.K., K.O.), Cardiovascular Medicine (T.I., H.M., K.S.), and Cell and Molecular Medicine (J.M., Y.S.), Jichi Medical University, Tochigi, Japan; the Department of Molecular Therapy (T.O.), National Institute of Neuroscience, National Center of Neurology and Psychiatry, Tokyo, Japan; and the Department of Organ Regeneration (M.T., U.I.), Shinshu University Graduate School of Medicine, Matsumoto, Japan.

Correspondence to Takayuki Ito or Keiya Ozawa, Division of Genetic Therapeutics, Jichi Medical University, 3311-1 Yakushiji, Shimotsuke, Tochigi 329-0498, Japan. E-mail titou@jichi.ac.jp or kozawa@jichi.ac.jp

Hypertension is available at http://hyper.ahajournals.org

DOI: 10.1161/HYPERTENSIONAHA.107.091348

Single subcutaneous injection of a pyrrolizidine alkaloid, namely, monocrotaline (MCT), produces severe PAH and PA remodeling in rats. We examined the effects of sustained PGIS expression in preventing PAH development and progression by means of this widely used model and an AAV1 vector.

Methods

Western Blot Analysis for PGIS Expression In Vitro

Human embryonic kidney 293 (HEK293) cells were incubated in 10-cm dishes containing DMEM and nutrient mixture F12 (Invitrogen) with 2% FCS in an atmosphere of 5% CO_2 in air at 37°C. The cells at 70% confluence were transfected with an AAV proviral plasmid encoding human PGIS (phPGIS, a kind gift from Dr Mimuro) or plasmid encoding enhanced green fluorescent protein (eGFP) by using a calcium phosphate method. The cells were harvested 72 hours after transfection, and cell lysates were prepared with a lysis buffer (10 mmol/L of Tris-HCl, 150 mmol/L of NaCl, and 1% NP40 [pH 7.6]) containing Complete Mini protease inhibitor (Roche Diagnostics). For Western blot analysis, 10 μg of the lysate was subjected to 10% SDS-PAGE and transferred to a nitrocellulose membrane. The membrane was blocked and incubated with a 1:500 dilution of rabbit anti-human PGIS polyclonal antibody (a gift from Dr Mimuro) and a 1:5000 dilution of peroxidase-linked anti-rabbit IgG antibody (Amersham Pharmacia Biotech), and immunoreactive bands were visualized using an enhanced chemiluminescence Western blotting kit (Amersham).

AAV-PGIS Production and PGI_2 Expression

We developed a recombinant AAV1-based vector containing the human PGIS or eGFP gene controlled by a modified chicken β-actin promoter with a cytomegalovirus immediate-early enhancer (AAV-PGIS or AAV-eGFP) to obtain efficient transgene expression in skeletal muscle cells. The AAV vectors were prepared according to the previously described 3-plasmid transfection adenovirus-free protocol with minor modifications for enabling the use of an active gassing system.[10,11] In brief, 60% confluent HEK293 cells that were incubated in a large culture vessel with active air circulation were cotransfected with phPGIS, AAV-1 chimeric helper plasmid (p1RepCap), and adenoviral helper plasmid pAdeno (Avigen Inc). The crude viral lysate was purified with 2 rounds of cesium chloride 2-tier centrifugation.[12] The titer of the viral stock was determined against plasmid standards by real-time PCR with primers 5′-CCCGCGAGGTTGTGGTGGAC-3′ and 5′-ATGGGCGGATGCG-GTAGC-3′; subsequently, the stock was dissolved in a buffer (50 mmol/L of HEPES [pH 7.4] and 0.15 mol/L of NaCl [HN buffer]) before infection. The HEK293 cells cultured in 6-well plates containing DMEM and nutrient mixture F12 with 5% FCS were infected with AAV-PGIS at 1×10^4 genome copies per cell to evaluate PGI_2 expression in vitro, and the supernatant was harvested after 72 hours. Concentrations of 6-keto-prostaglandin $F_{1\alpha}$ (6-keto-$PGF_{1\alpha}$) in plasma or culture media were determined by enzyme immunoassay (R&D Systems) according to the manufacturer's instructions. The minimum detectable dose of the assay was <1.4 pg/mL. Interassay and intra-assay precision of the kit was <10%.

Animal Models

All of the animal experiments were approved by the Jichi Medical University ethics committee and were performed in accordance with the National Institutes of Health Guide for the Care and Use of Laboratory Animals. To evaluate the efficiency of gene expression in vivo, AAV-eGFP (200 μL; 1×10^{11} gene copies per body) or AAV-PGIS (200 μL: 1×10^{10} to 1×10^{11} gene copies per body) was injected into the bilateral anterior tibial muscles (n=3 each) of 3-week–old male Wistar rats (Clea Japan Inc) weighing 45 to 55 g. For hemodynamics and histological analyses, the rats were divided into 4 groups: sham rats that were administered the HN buffer (group 1, negative control [NC] group; n=4); MCT-PAH rats administered the HN buffer (group 2, MCT group; n=6); MCT rats administered AAV-eGFP (group 3, MCT+eGFP group; n=6); and MCT rats administered AAV-PGIS (group 4, MCT+PGIS group; n=10). After the anesthesia with spontaneous inhalation of 1% isoflurane, the rats in groups 3 and 4 were intramuscularly injected with AAV-eGFP or AAV-PGIS (1×10^{10} gene copies per body), whereas those in groups 1 and 2 were injected with the HN buffer (200 μL). MCT (Wako Pure Chemicals) was dissolved in 0.1 N HCl, and the pH was adjusted to 7.4 with 1.0 N NaOH. After the anesthesia with spontaneous inhalation of 1% isoflurane, all of the rats except for those in the NC group were injected subcutaneously with MCT (40 mg/kg) 4 weeks after the injecting the vector. Blood samples were collected from the tail vein on ethylenediamine tetraacetic acid tubes, and the concentrations of the leukocytes, platelets, hematocrit, alanine aminotransferase, and creatinine were determined by standard procedures.

Hemodynamics Analysis

Four weeks after the MCT injection, the rats were anesthetized with spontaneous inhalation of 1% isoflurane, and a tracheotomy was performed. Then, they were mechanically ventilated with 1% isoflurane (tidal volume, 10 mL/kg; respiratory rate, 30 breaths per minute) through a tracheostomy. After the thoracic cavity was opened using a midsternal approach, 2F high-fidelity manometer-tipped catheters (SPC-320; Millar Instruments Inc) were inserted directly into the right or left ventricle, and an ultrasonic flow probe (flow probe 2.5S176; Transonic Systems Inc) was placed on the ascending root of the aorta. The heart rate, mean pulmonary arterial pressure (mPAP), aortic systolic arterial pressure, left ventricular end-diastolic pressure (LVEDP), and mean aortic flow indicating the cardiac output (CO) were measured. Cardiac indices (CI) and pulmonary vascular resistance (PVR) were calculated using the following formula: $CI\ (mL\cdot min^{-1}\cdot kg^{-1})=CO/body\ weight$, $PVR\ (mm\ Hg\cdot mL^{-1}\cdot min^{-1}\cdot kg^{-1})=(mPAP-LVEDP)/CI$.

Ventricular Weight Measurement and Morphometric Analysis of the PA

After the hemodynamic analysis, the rats were killed with an overdose (5%) of isoflurane through a tracheostomy. Their lungs were perfused with 5 mL of saline followed by 10 mL of cold 4% paraformaldehyde. Each ventricle and the lungs were then excised, dissected free, and weighed. The weight ratio of the right ventricle to the left ventricle plus septum [RV/(LV+S)] was calculated as an index of right ventricular hypertrophy (RVH). The lung tissues were fixed overnight at 4°C in 4% paraformaldehyde and frozen in Tissue-Tek OCT compound (Sakura Finetechnical Co) at −20°C. Hematoxylin and eosin staining was performed on 7-μm–thick sections that were subsequently examined using light microscopy. A morphometric analysis was performed on a PA having an external diameter of 25 to 50 μm or 51 to 100 μm. The medial wall thickness was calculated using the following formula: medial thickness (%)=medial wall thickness/external diameter×100.[13] For the quantitative analysis, 30 vessels of each rat were measured and averaged randomly by the 2 external observers.

Survival Analysis

The 3-week–old Wistar rats were divided into 3 groups (MCT, MCT+eGFP, and MCT+PGIS; n=8 each). After the anesthesia with spontaneous inhalation of 1% isoflurane, the rats in the MCT+eGFP or MCT+PGIS group were intramuscularly injected with AAV-eGFP or AAV-PGIS at 1×10^{10} genome copies per body, respectively. Under the same anesthetic condition, all of the rats were injected subcutaneously with MCT (40 mg/kg) at 4 weeks after injecting the vector. The survival rate was estimated from the date of the MCT administration until death or after 8 weeks of the injection. Survival curves were analyzed using the Kaplan-Meier method and compared by log-rank tests.

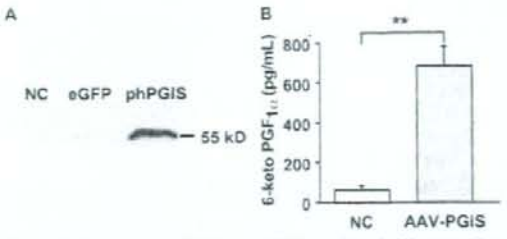

Figure 1. Expression of PGIS and PGI_2 in vitro. A, Western blot analysis of PGIS expression in HEK293 cells after plasmid transfection. The cells were harvested 72 hours after transfection with phPGIS or eGFP. B, AAV vector-mediated PGI_2 expression in HEK293 cells. The PGI_2 levels were estimated by measuring the amount of 6-keto-$PGF_{1\alpha}$, a stable metabolite of PGI_2, in the culture supernatant by enzyme immunoassay 72 hours after infecting the cells (n=4 each) with AAV-PGIS (1×10^4 genome copies per cell). Data are presented as mean±SEM. $^{**}P<0.01$. NC indicates untreated negative control.

Statistical Analysis

The statistical analysis and correlations were performed using StatView (Abacus Concepts, Inc). Data are presented as mean±SEM. Differences in parameters were evaluated using ANOVA combined with Fisher's test. A value of $P<0.05$ was considered statistically significant.

Results

Expression of PGIS and PGI_2 In Vitro

Western blot analysis revealed that transfection of the HEK293 cells with phPGIS but not with a plasmid carrying the eGFP gene enhanced the production of the PGIS protein (Figure 1A). Infection of the cells with AAV-PGIS at 1×10^4 genome copies per cell significantly increased the concentration of 6-keto-$PGF_{1\alpha}$, a stable metabolite of PGI_2, in culture supernatants as compared with that without vector infection (Figure 1B).

AAV Vector-Mediated Systemic PGI_2 Expression in the Rats

Four weeks after the injection of AAV vectors (1×10^{10} genome copies per body), the PGIS-transduced rats began exhibiting significant increases in the plasma 6-keto-$PGF_{1\alpha}$ levels as compared with the control rats (Figure 2A). Eight weeks after the injection, the 6-keto-$PGF_{1\alpha}$ levels increased further in a vector dose-dependent manner in the treated rats (Figure 2B) as compared with the untreated controls (6.68±1.33 versus 1.62±0.30 ng/mL, 1×10^{11} versus 1×10^{10} genome copies per body, respectively; $P<0.05$; n=3 each). The vectors at 1×10^{10} genome copies per body were used for all of the subsequent experiments. In contrast, injection of 1×10^{11} genome copies per body of AAV-eGFP produced no significant change in the 6-keto-$PGF_{1\alpha}$ levels.

Effects of PGI_2 Expression on Hemodynamics and RVH

Four weeks after the MCT administration, the mPAP levels were significantly elevated in the treated rats as compared with the untreated controls (Figure 3A). Treatment with AAV-PGIS but not AAV-eGFP significantly inhibited this increase (Figure 3A). In addition, the expression of PGI_2

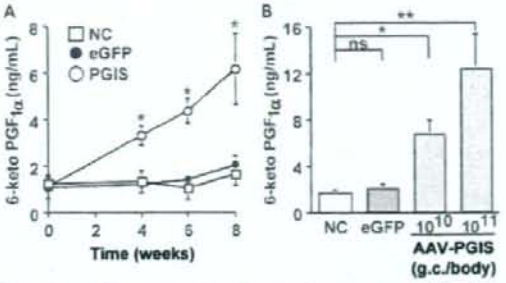

Figure 2. AAV vector-mediated systemic expression of PGI_2 in vivo. The concentration of plasma 6-keto-$PGF_{1\alpha}$ was determined by enzyme immunoassay after a single injection of AAV-PGIS into the anterior tibial muscle of 3-week-old male Wistar rats. A, Time course of plasma 6-keto-$PGF_{1\alpha}$ levels after injection of AAV-PGIS at 1×10^{10} genome copies per body. B, Vector dose dependency of plasma 6-keto-$PGF_{1\alpha}$ levels 8 weeks after the injection. The rats injected with AAV-eGFP (1×10^{11} genome copies per body) were used as controls. Data are presented as mean±SEM (n=3 animals per group). ns indicates not statistically significant; NC, untreated negative control. $^{*}P<0.05$ vs NC; $^{**}P<0.01$.

significantly mitigated an increase in PVR and a decrease in CI that were induced by MCT (Figure 3B and 3C, respectively); however, it produced no significant changes in the heart rate and aortic systolic arterial pressure (Table). PGI_2 expression also had a beneficial effect on RVH. Treatment with AAV-PGIS but not AAV-eGFP significantly inhibited the MCT-induced increase in RV/(LV+S) (Figure 3D).

Effects on Medial Hypertrophy of the PA

Medial hypertrophy is a hallmark of pathological vascular remodeling in PAH. Four weeks after the MCT injection, the

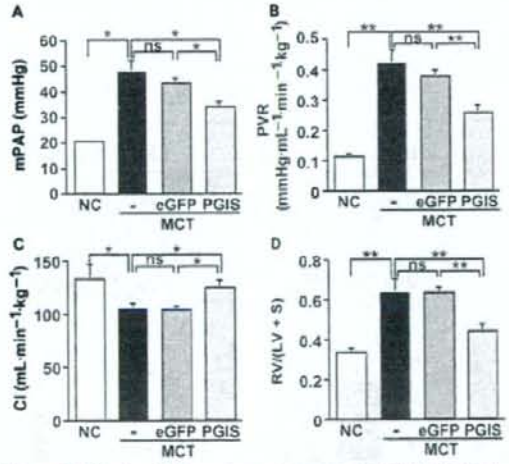

Figure 3. Effects of PGI_2 on hemodynamics and RVH. A quantitative analysis was performed using MCT-induced PAH rats 8 weeks after injecting the vector. A, mPAP (mm Hg); B, PVR (mm Hg · mL^{-1} · min^{-1} · kg^{-1}); C, CI (mL · min^{-1} · kg^{-1}). D, Weight ratio of the right ventricle to the left ventricle plus septum [RV/(LV+S)] presented as an index of RVH. Data are presented as means±SEM (n=4 to 10 animals per group). $^{*}P<0.05$; $^{**}P<0.01$. ns indicates not statistically significant; NC, untreated negative control.

Physiological and Laboratory Data of the MCT-Induced PAH Rats

Factor	NC	MCT	MCT + eGFP	MCT + PGIS	*P*
No. of rats	4	6	6	10	...
Heart rate, per minute	294.0±10.6	281.2±14.7	268.0±9.0	274.8±8.7	NS
ASAP, mm Hg	99.5±1.6	97.3±2.0	96.3±2.4	94.7±4.4	NS
Body weight, g	358.5±11.5	328.3±7.2	328.0±11.4	342.5±9.8	NS
Leukocyte, per mL	6725±372	7917±723	8800±849	8030±852	NS
Hematocrit, %	48.2±0.7	48.9±1.9	51.0±3.0	47.8±1.8	NS
Platelet, $\times 10^4/mm^2$	88.3±8.7	79.2±8.8	80.4±3.6	84.6±6.3	NS
ALT, IU/L	37.8±2.5	49.5±8.4	52.5±6.8	44.1±4.3	NS
Cr, mg/dL	0.52 0.04	0.59 0.05	0.48 0.03	0.53 0.04	NS

Data are presented as means±SEM (n=4 to 10 animals per group). ASAP indicates aortic systolic arterial pressure; ALT, serum alanine aminotransferase; Cr, serum creatinine; NS, not statistically significant.

medial thickness of the PA was greater in the MCT-administered rats than in the untreated controls (Figure 4A). Treatment with AAV-PGIS but not AAV-eGFP prevented the MCT-induced increase in the percentage of medial thickness significantly (Figure 4B, 25 to 50 μm; Figure 4C, 51 to 100 μm in external diameter).

Effects on the Survival of the MCT-PAH Rats and Their Organ Dysfunctions

The PGIS-transduced rats exhibited significantly improved survival rates as compared with the eGFP-transduced rats (Figure 5). The MCT administration produced a slight but not significant decrease in the body weight of the rats, and PGIS gene transfer prevented this decrease. Although the MCT group showed only a slight but not significant increase in the leukocyte count and serum alanine aminotransferase levels as compared with the NC group, the AAV-PGIS treatment caused no additional change in these parameters (Table).

Discussion

The present study demonstrates that sustained PGI_2 expression by a single intramuscular injection of AAV-PGIS prevents the development of MCT-PAH in rats. PGI_2 expression not only increased the cardiac output significantly but also prevented the progression of PVR, RVH, and medial hypertrophy of the PA that was induced by the MCT administration. The PGIS-transduced rats also exhibited significantly improved survival rates as compared with the controls. Furthermore, the PGIS expression observed in this study caused no additional adverse effects on hematologic data and serum indicators of hepatorenal function (alanine aminotransferase and creatinine levels) in the MCT-PAH rats.

The expression of PGI_2 and PGIS decreased in the remodeled PAs of the idiopathic PAH patients.[14,15] Impaired PGI_2 synthesis resulting from a decrease in PGIS expression may be implicated in the pathogenesis of PAH. In fact, continuous intravenous infusion of exogenous PGI_2 markedly lowers PVR and improves survival in PAH patients. However, this system requires lifelong infusion with a central venous catheter because of the short biological half-life of PGI_2. Furthermore, because this system is associated with life-threatening complications (eg, shock and sepsis) that may result in poor survival and quality of life of patients, stable

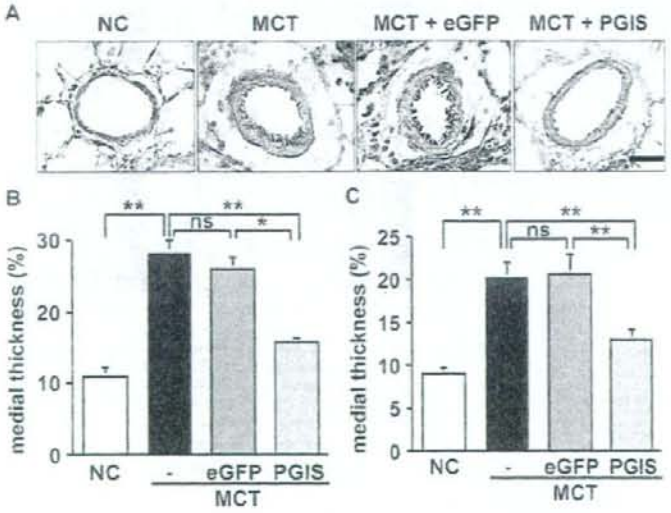

Figure 4. Effects of PGI_2 on medial hypertrophy of the peripheral PA. A, Representative cross-sections of the peripheral PA 4 weeks after the MCT administration (hematoxylin and eosin staining, original magnification, ×1000; scale bar=20 μm). B and C, Quantitative analysis of percentage of medial thickness (B, 25 to 50 μm; C, 51 to 100 μm in external diameter). Data are presented as means±SEM (n=4 to 10 animals per group). *$P<0.05$, **$P<0.01$. ns indicates not statistically significant; NC, untreated negative control.

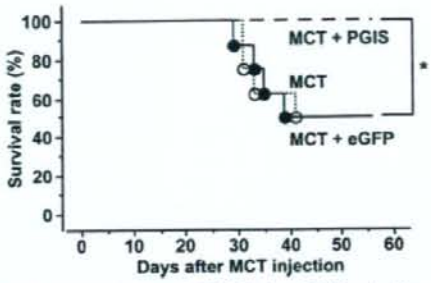

Figure 5. The survival rate of MCT-induced PAH rats. The rats were administered with MCT (40 mg/kg) 4 weeks after the injection of HN buffer (MCT group), AAV-eGFP (MCT+eGFP group), or AAV-PGIS (MCT+PGIS group). The rats were intramuscularly injected with the vectors at 1×10^{10} genome copies per body. The Kaplan-Meier method demonstrated a significant improvement in the survival rate of the rats in the MCT+PGIS group as compared with those in either the MCT or MCT+eGFP group at 8 weeks post-MCT administration. n=8 animals per group; *$P<0.05$ vs MCT or eGFP groups.

production of endogenous PGI_2 would be more desirable. Consistent with previous gene therapy studies, our strategy presented high levels of endogenous PGI_2 expression. In addition, this strategy caused no systemic hypotension and hyperdynamic heart failure, which are the major adverse effects arising from uncontrolled blood levels during intravenous delivery of exogenous PGI_2.[3,4,6]

In this study, we used an AAV serotype 1 vector because it is effective not only in efficient muscle transduction but also in long-term secretion of therapeutic proteins into the systemic circulation. The cDNA for human PGIS shares a high identity with its rat counterpart.[16] In fact, the administration of a plasmid or hemagglutinating virus of the Japan-liposome vector encoding human PGIS successfully ameliorated MCT-PAH. However, the use of these vectors requires repeated administration for achieving sustained gene expression.[3-5] In contrast, the AAV vector used in this study achieved PGIS expression with a single intramuscular injection, and this expression was sustained for 1 year.[7]

Furthermore, gene transfer was believed to be safer when performed via an intramuscular approach as opposed to the intratracheal or intrahepatic approaches.[6] Currently, researchers are using adenoviral gene transfer in most clinical trials because of its high efficiency for gene expression. However, the potential toxic effects of adenoviruses, such as strong immunogenicity, are well known. In contrast, the intramuscular administration of AAV vectors is a promising strategy for delivering therapeutic proteins safely and efficiently, and their use has been examined in clinical trials for hemophilia.[17]

Although PGI_2 is known to be a short-acting vasodilator, recent studies have shown its antiremodeling effects when used in high doses. The administration of PGI_2 analogues cicaprost and iloprost in high concentrations ($>10^{-7}$ mol/L) inhibits mitogen-induced proliferation of rat primary PA smooth muscle cells in a cAMP-dependent manner.[18] Interestingly, another PGI_2 analogue, treprostinil, also inhibits the proliferation of human and mouse primary lung fibroblasts through the activation of a peroxisome proliferator-activated receptor-β/δ when used in equivalent doses.[19] These observations suggest that high levels of PGI_2 may attenuate PA remodeling in vivo through antiproliferative effects. Consistent with previous studies, we demonstrated that high levels of endogenous PGI_2 successfully attenuated medial hypertrophy of the PA.[3,4,6] To discover new drug targets, the roles of peroxisome proliferator-activated receptors and high-level PGI_2 in PAH therapy should be determined, because peroxisome proliferator-activated receptors are associated with many inflammatory and proliferative disorders, including PAH.[2,20]

Finally, we will discuss the clinical implications and limitations of this study. Consistent with previous studies, maximum gene expression was noted 6 to 8 weeks after the intramuscular injection of AAV vectors. AAV-PGIS was injected 4 weeks before MCT administration for the transgene expression to reach plateau levels when MCT-PAH was fully developed (3 to 4 weeks after the injection). Our results are completely based on a preventive protocol, which may be rare in a clinical setting. However, PGI_2 is an established therapeutic molecule, and the advantage of early initiation of PGI_2 therapy for improving survival in patients with idiopathic PAH has been demonstrated in a large clinical trial.[21] These observations convinced us to propose the possible preemptive use of AAV-PGIS as a strategy to maintain basal levels of PGI_2 in patients with mild symptoms of PAH or in those identified as high-risk subjects who have not experienced PAH. As an alternative, the combined use of AAV-PGIS and an initial infusion of intravenous PGI_2 might be promising; the intravenous infusion should be tapered when sufficient levels of PGI_2 are attained. To evaluate the efficacy of AAV-PGIS in a therapeutic protocol (ie, vector injection after the development of PAH), use of a chronic hypoxic PAH model or newly developed self-complementary AAV vectors that can express transgenes earlier than the conventional vectors should be considered.[22]

Perspectives

The present study has demonstrated that the single intramuscular injection of AAV-PGIS achieved a sustained expression of PGI_2. This expression retarded the progression of MCT-PAH in rats without causing significant adverse effects. Thus, this strategy provides a new therapeutic alternative for PAH patients. However, the system in this study lacks the ability to regulate excessive transgene expression. Therefore, regulatory mechanisms to ensure adequate gene expression should be established to facilitate successful translation of this strategy in a clinical setting.

Acknowledgment

We thank Miyoko Mitsu for her encouragement and technical support.

Sources of Funding

This work was supported in part by grants from the Ministry of Health, Labor and Welfare of Japan; Grants-in-Aid for Scientific Research; grant for the 21st Century Centes of Excellence Program; "High-Tech Research Center" Project for Private Universities, matching fund subsidy, from the Ministry of Education, Culture,

Sports, Science and Technology of Japan; and the Research Award to Jichi Medical School Graduate Student.

Disclosures

None.

References

1. Humbert M, Sitbon O, Simonneau G. Treatment of pulmonary arterial hypertension. *N Engl J Med*. 2004;351:1425–1436.
2. Ito T, Ozawa K, Shimada K. Current drug targets and future therapy of pulmonary arterial hypertension. *Curr Med Chem*. 2007;14:719–733.
3. Nagaya N, Yokoyama C, Kyotani S, Shimonishi M, Morishita R, Uematsu M, Nishikimi T, Nakanishi N, Ogihara T, Yamagishi M, Miyatake K, Kaneda Y, Tanabe T. Gene transfer of human prostacyclin synthase ameliorates monocrotaline-induced pulmonary hypertension in rats. *Circulation*. 2000;102:2005–2010.
4. Suhara H, Sawa Y, Fukushima N, Kagisaki K, Yokoyama C, Tanabe T, Ohtake S, Matsuda H. Gene transfer of human prostacyclin synthase into the liver is effective for the treatment of pulmonary hypertension in rats. *J Thorac Cardiovasc Surg*. 2002;123:855–861.
5. Ono M, Sawa Y, Mizuno S, Fukushima N, Ichikawa H, Bessho K, Nakamura T, Matsuda H. Hepatocyte growth factor suppresses vascular medial hyperplasia and matrix accumulation in advanced pulmonary hypertension of rats. *Circulation*. 2004;110:2896–2902.
6. Tahara N, Kai H, Niiyama H, Mori T, Sugi Y, Takayama N, Yasukawa H, Numaguchi Y, Matsui H, Okumura K, Imaizumi T. Repeated gene transfer of naked prostacyclin synthase plasmid into skeletal muscles attenuates monocrotaline-induced pulmonary hypertension and prolongs survival in rats. *Hum Gene Ther*. 2004;15:1270–1278.
7. Yoshioka T, Okada T, Maeda Y, Ikeda U, Shimpo M, Nomoto T, Takeuchi K, Nonaka-Sarukawa M, Ito T, Takahashi M, Matsushita T, Mizukami H, Hanazono Y, Kume A, Ookawara S, Kawano M, Ishibashi S, Shimada K, Ozawa K. Adeno-associated virus vector-mediated interleukin-10 gene transfer inhibits atherosclerosis in apolipoprotein E-deficient mice. *Gene Ther*. 2004;11:1772–1779.
8. Chen S, Kapturczak MH, Wasserfall C, Glushakova OY, Campbell-Thompson M, Deshane JS, Joseph R, Cruz PE, Hauswirth WW, Madsen KM, Croker BP, Berns KI, Atkinson MA, Flotte TR, Tisher CC, Agarwal A. Interleukin 10 attenuates neointimal proliferation and inflammation in aortic allografts by a heme oxygenase-dependent pathway. *Proc Natl Acad Sci U S A*. 2005;102:7251–7256.
9. Mu W, Ouyang X, Agarwal A, Zhang L, Long DA, Cruz PE, Roncal CA, Glushakova OY, Chiodo VA, Atkinson MA, Hauswirth WW, Flotte TR, Rodriguez-Iturbe B, Johnson RJ, IL-10 suppresses chemokines, inflammation, and fibrosis in a model of chronic renal disease. *J Am Soc Nephrol*. 2005;16:3651–3660.
10. Matsushita T, Elliger S, Elliger C, Podsakoff G, Villarreal L, Kurtzman GJ, Iwaki Y, Colosi P. Adeno-associated virus vectors can be efficiently produced without helper virus. *Gene Ther*. 1998;5:938–945.
11. Okada T, Nomoto T, Yoshioka T, Nonaka-Sarukawa M, Ito T, Ogura T, Iwata-Okada M, Uchibori R, Shimazaki K, Mizukami H, Kume A, Ozawa K. Large-scale production of recombinant viruses by use of a large culture vessel with active gassing. *Hum Gene Ther*. 2005;16:1212–1218.
12. Okada T, Nomoto T, Shimazaki K, Lijun W, Lu Y, Matsushita T, Mizukami H, Urabe M, Hanazono Y, Kume A, Muramatsu S, Nakano I, Ozawa K. Adeno-associated virus vectors for gene transfer to the brain. *Methods*. 2002;28:237–247.
13. Kay JM, Keane PM, Suyama KL, Gauthier D. Angiotensin converting enzyme activity and evolution of pulmonary vascular disease in rats with monocrotaline pulmonary hypertension. *Thorax*. 1982;37:88–96.
14. Christman BW, McPherson CD, Newman JH, King GA, Bernard GR, Groves BM, Loyd JE. An imbalance between the excretion of thromboxane and prostacyclin metabolites in pulmonary hypertension. *N Engl J Med*. 1992;327:70–75.
15. Tuder RM, Cool CD, Geraci MW, Wang J, Abman SH, Wright L, Badesch D, Voelkel NF. Prostacyclin synthase expression is decreased in lungs from patients with severe pulmonary hypertension. *Am J Respir Crit Care Med*. 1999;159:1925–1932.
16. Miyata A, Hara S, Yokoyama C, Inoue H, Ullrich V, Tanabe T. Molecular cloning and expression of human prostacyclin synthase. *Biochem Biophys Res Commun*. 1994;200:1728–1734.
17. High K. AAV-mediated gene transfer for hemophilia. *Genet Med*. 2002; 4:56S–61S.
18. Phillips PG, Long L, Wilkins MR, Morrell NW. cAMP phosphodiesterase inhibitors potentiate effects of prostacyclin analogs in hypoxic pulmonary vascular remodeling. *Am J Physiol Lung Cell Mol Physiol*. 2005;288: L103–L115.
19. Ali FY, Egan K, FitzGerald GA, Desvergne B, Wahli W, Bishop-Bailey D, Warner TD, Mitchell JA. Role of prostacyclin versus peroxisome proliferator-activated receptor beta receptors in prostacyclin sensing by lung fibroblasts. *Am J Respir Cell Mol Biol*. 2006;34:242–246.
20. Ameshima S, Golpon H, Cool CD, Chan D, Vandivier RW, Gardai SJ, Wick M, Nemenoff RA, Geraci MW, Voelkel NF. Peroxisome proliferator-activated receptor gamma (PPARgamma) expression is decreased in pulmonary hypertension and affects endothelial cell growth. *Circ Res*. 2003;92:1162–1169.
21. Sitbon O, Humbert M, Nunes H, Parent F, Garcia G, Herve P, Rainisio M, Simonneau G. Long-term intravenous epoprostenol infusion in primary pulmonary hypertension: prognostic factors and survival. *J Am Coll Cardiol*. 2002;40:780–788.
22. Nathwani AC, Gray JT, McIntosh J, Ng CY, Zhou J, Spence Y, Cochrane M, Gray E, Tuddenham EG, Davidoff AM. Safe and efficient transduction of the liver after peripheral vein infusion of self-complementary AAV vector results in stable therapeutic expression of human FIX in nonhuman primates. *Blood*. 2007;109:1414–1421.

Interleukin-10 Expression Mediated by an Adeno-Associated Virus Vector Prevents Monocrotaline-Induced Pulmonary Arterial Hypertension in Rats

Takayuki Ito, Takashi Okada, Hiroshi Miyashita, Tatsuya Nomoto, Mutsuko Nonaka-Sarukawa, Ryosuke Uchibori, Yoshikazu Maeda, Masashi Urabe, Hiroaki Mizukami, Akihiro Kume, Masafumi Takahashi, Uichi Ikeda, Kazuyuki Shimada, Keiya Ozawa

Abstract—Pulmonary arterial hypertension (PAH) is a fatal disease associated with inflammation and pathological remodeling of the pulmonary artery (PA). Interleukin (IL)-10 is a pleiotropic antiinflammatory cytokine with vasculoprotective properties. Here, we report the preventive effects of IL-10 on monocrotaline-induced PAH. Three-week-old Wistar rats were intramuscularly injected with an adeno-associated virus serotype 1 vector expressing IL-10, followed by monocrotaline injection at 7 weeks old. IL-10 transduction significantly improved survival rates of the PAH rats 8 weeks after monocrotaline administration compared with control gene transduction (75% versus 0%, $P<0.01$). IL-10 also significantly reduced mean PA pressure (22.8 ± 1.5 versus 29.7 ± 2.8 mm Hg, $P<0.05$), a weight ratio of right ventricle to left ventricle plus septum (0.35 ± 0.04 versus 0.42 ± 0.05, $P<0.05$), and percent medial thickness of the PA ($12.9\pm0.3\%$ versus $21.4\pm0.4\%$, $P<0.01$) compared with controls. IL-10 significantly reduced macrophage infiltration and vascular cell proliferation in the remodeled PA in vivo. It also significantly decreased the lung levels of transforming growth factor-β_1 and IL-6, which are indicative of PA remodeling. In addition, IL-10 increased the lung level of heme oxygenase-1, which strongly prevents PA remodeling. In vitro analysis revealed that IL-10 significantly inhibited excessive proliferation of cultured human PA smooth muscle cells treated with transforming growth factor-β_1 or the heme oxygenase inhibitor tin protoporphyrin IX. Thus, IL-10 prevented the development of monocrotaline-induced PAH, and these results provide new insights into the molecular mechanisms of human PAH. (***Circ Res.*** **2007;101:734-741.)**

Key Words: pulmonary hypertension ■ interleukins ■ gene therapy ■ inflammation ■ vascular smooth muscle cell proliferation

Pulmonary arterial hypertension (PAH) is an intractable disease that leads to increased pulmonary arterial pressure, progressive right heart failure, and premature death; however, no satisfactory treatment for PAH has been established.[1] The pathological process of PAH is characterized by abnormal remodeling of the pulmonary artery (PA) associated with excessive proliferation of pulmonary arterial smooth muscle cells (PASMCs).[2] Accumulating evidence suggests important roles of vascular inflammation in its pathogenesis.[2,3] For instance, serum levels of proinflammatory cytokines such as interleukin (IL)-1 and IL-6 reflect the disease activity in patients with idiopathic PAH.[4] Furthermore, injection of IL-6 can produce PAH and PA remodeling in rats.[5] The remodeled PA presents macrophage infiltration and increased expression of a variety of cytokines, including IL-6, tumor necrosis factor (TNF)-α, and transforming growth factor (TGF)-β_1.[6,7] Administration of steroids or immunosuppressive drugs decreases the level of PA pressure in patients with PAH.[8,9] These observations suggest a therapeutic potential of targeting inflammation to prevent PAH progression.[10] However, the precise mechanisms underlying the antiinflammatory effects on PA remodeling have not yet been fully investigated.

IL-10 is a multifunctional antiinflammatory cytokine with a vasculoprotective property. During the course of inflammation, IL-10 is produced by type-2 helper T (Th2) lymphocytes, and it inhibits the production of various proinflammatory cytokines in macrophages and Th1 lymphocytes.[11] Exogenous IL-10 prevents proliferative vasculopathy in vivo by inhibiting inflammatory cell infiltration,[12] smooth muscle cell proliferation,[12,13] and chemokine expression.[14] However, clinical efficacy of systemic recombinant IL-10 administra-

Original received March 28, 2007; revision received July 12, 2007; accepted July 23, 2007.

From the Division of Genetic Therapeutics (T.I., T.N., M.N.-S., M.U., H.M., A.K., K.O., R.U.), the Division of Cardiovascular Medicine (T.I., H.M., M.N.-S., K.S., Y.M.), Jichi Medical University, Japan; the Department of Molecular Therapy (T.O.), National Institute of Neuroscience, National Center of Neurology and Psychiatry, Japan; and the Department of Organ Regeneration (M.T., U.I.), Shinshu University Graduate School of Medicine, Japan.

Correspondence to Takayuki Ito, MD, PhD, Division of Genetic Therapeutics, Jichi Medical University, 3311-1 Yakushiji, Shimotsuke, Tochigi 329-0498, Japan. E-mail utou@jichi.ac.jp

Circulation Research is available at http://circres.ahajournals.org

DOI: 10.1161/CIRCRESAHA.107.153023

tion are insufficient because of the lower local IL-10 levels resulting from its short bioactive half-life.[15] In this study, we used an adeno-associated virus (AAV) vector for IL-10 expression because it is an efficient vehicle for systemic and sustained expression of therapeutic proteins.[14] It also has an advantage over other viral vectors in the therapeutic or mechanistic analysis because it produces minimal inflammatory and immune responses in vivo.

Recently, heme oxygenase (HO)-1, an inducible form of HO that promotes production of a vasodilator carbon monoxide (CO), was shown to mediate antiinflammatory and antiproliferative effects of IL-10 in a model of chronic vasculopathy.[12] Increased HO-1 and CO levels attenuated PAH and PA remodeling by inhibiting PASMC proliferation.[16–18] However, no study has explored a direct link between IL-10 and HO-1 in the pathogenesis of PAH. Thus, we examined the effects of IL-10, delivered via an AAV vector, on PA remodeling in a widely-used rat model of PAH induced by the pyrolizidine alkaloid monocrotaline (MCT). We also investigated the mechanisms underlying the effects of IL-10 on the following factors involved in the inflammatory and proliferative vascular changes in PAH: PASMC, macrophage, TGF-β_1, IL-6, and HO-1.

Materials and Methods

AAV Vector Production

DNA encoding rat IL-10 was polymerase chain reaction-amplified from rat splenocyte complementary DNA, using the primers 5′-GCACGAGAGCCACAACGCA-3′ and 5′-GATTTGAGTACG-ATCCATTTATTCAAAACGAGGAT-3′. For efficient transgene expression in the skeletal muscle, we constructed a recombinant AAV vector which carried the IL-10 gene (AAV-IL-10) or enhanced green fluorescent protein (eGFP) gene (AAV-eGFP), controlled by the modified chicken β-actin promoter with the cytomegalo virus-immediate early enhancer and the woodchuck hepatitis virus post-transcriptional regulatory element (a kind gift from Dr Thomas Hope, Infectious Disease Laboratory, Salk Institute). AAV vectors were prepared according to the previously described 3-plasmid transfection adenovirus-free protocol with minor modifications to use the active gassing system.[19,20] In brief, 60% confluent human embryonic kidney 293 cells incubated in a large culture vessel with active air circulation were cotransfected with the proviral transgene plasmid, AAV-1 chimeric helper plasmid (p1RepCap), and adenoviral helper plasmid pAdeno (Avigen Inc). The crude viral lysate was purified by 2 rounds of cesium chloride 2-tier centrifugation.[21] The viral stock titer was determined against plasmid standards by dot blot hybridization, after which the stock was dissolved in HN buffer (50 mmol/L HEPES, pH 7.4, 0.15 mol/L NaCl) before injection.

Animal Models

All animal experiments were approved by the Jichi Medical University ethics committee and were performed in accordance with the *National Institute of Health Guide for the Care and Use of Laboratory Animals*. To evaluate the efficiency of in vivo gene expression, 3-week-old male Wistar rats (Clea Japan Inc, Tokyo, Japan) weighing 45 to 55 g were injected with AAV-IL-10 (200 μL, 3×10^{10} to 1×10^{11} genome copies [g.c.] per body) into the bilateral anterior tibial muscles (n=3 animals per group). For hemodynamic and histological analysis, we randomly formed 4 groups comprising 5 rats each: sham rats that were administered the HN buffer (1, NC group); MCT-treated rats administered the HN buffer (2, MCT group); MCT rats administered AAV-eGFP (3, MCT+eGFP group); and MCT rats administered AAV-IL-10 (4, MCT+IL-10 group). After anesthetized with a spontaneous inhalation of 1% isoflurane, the rats in the groups 3 and 4 received intramuscular injection of AAV-eGFP or AAV-IL-10 (200 μL, 6×10^{10} g.c. per body), respectively. Rats in groups 1 and 2 were injected with the HN buffer (200 μL). MCT (Wako Pure Chemicals) was dissolved in 0.1N HCl, and the pH adjusted to 7.4 with 1.0N NaOH. For hemodynamic and histological studies, all rats except those in the NC group were subcutaneously injected with MCT (30 mg/kg) under the spontaneous inhalation of 1% isoflurane at 4 weeks after vector treatment. For the survival study, rats (n=8 animals/group) were injected with a lethal dose of MCT (45 mg/kg) under the spontaneous inhalation of 1% isoflurane at 4 weeks after vector injection. Survival was estimated from the date of MCT injection until death or 8 weeks after injection.

Hemodynamic Analysis

Four weeks after MCT injection, the rats were anesthetized with spontaneous inhalation of 1% isoflurane, and a tracheotomy was performed. Then, they were mechanically ventilated using a respirator (SAR-830/AP, CWE; tidal volume: 10 mL/kg, respiratory rate: 30 breaths per min) and anesthetized with 0.5% isoflurane through a tracheostomy. After the thoracic cavity was opened using a midsternal approach, 2.0F high-fidelity manometer-tipped catheters (SPC-320, Millar Instruments Inc) were inserted directly into the right or left ventricle. The mean pulmonary arterial pressure (mPAP) or mean aortic arterial pressure (mAoP) was measured using the catheters that were advanced from the right or left ventricle, respectively. The heart rate (HR) was measured by unipolar lead electrocardiography.

Ventricular Weight Measurement and Morphometric Analysis of the PA

After hemodynamic analysis, the rats were euthanized using an overdose isoflurane (5%). The lungs and PAs were perfused with 5 mL of saline followed by 10 mL of cold 4% paraformaldehyde. Each ventricle and the lungs were excised, dissected free, and weighed. The weight ratio of right ventricle to the left ventricle plus septum [RV/(LV+S)] was calculated as an index of right ventricular hypertrophy (RVH). The tissues were fixed in 4% paraformaldehyde for 4 hours, transferred to 30% sucrose in 0.1 mol/L phosphate buffer (pH 7.4) for cryoprotection, and stored at 4°C overnight. Lung tissue was frozen in Tissue-Tek OCT compound (Sakura Finetechnical Co) at −20°C. Then, 7-μm sections were cut using a cryostat. Hematoxylin and eosin (HE) staining was performed on sections from the middle lobe of the right lung, and these were examined using light microscopy. Morphometric analysis was performed in PAs with an external diameter of 25 to 50 and 51 to 100 μm. The medial wall thickness was calculated with the following formula: medial thickness (%)=medial wall thickness/external diameter×100.[22] For quantitative analysis, 30 vessels from each rat were counted and the average was calculated.

Immunohistochemistry

Immunohistochemical staining was performed with monoclonal antibodies against ED1 (1:100; Serotec) and proliferating cell nuclear antigen (PCNA, 1:200; Zymed), using the streptavidin-biotin-peroxidase method, as described previously.[23] ED1 recognizes the lysosomal membrane antigen expressed by a majority of tissue macrophages. Irrelevant mouse immunoglobulin G (Vector Laboratories) was used as a negative control. Reactions were visualized using Vector SG (Vector Laboratories) or 3,3′-diaminobenzidine (Zymed) and counterstained with nuclear fast red or hematoxylin. The number of ED1-positive cells was counted in 250×250-μm fields under 400× magnification and expressed as cells per mm^2. The number of PCNA-positive cells was quantitatively evaluated as a percentage of total vascular cells in the fields under 1000× magnification. For each rat, the average number or percentage of each cell in 15 randomly selected fields was used for statistical analysis.

Protein Assay

Protein samples were prepared by homogenization of the frozen lung tissue in lysis buffer [10 μmol/L Tris/Cl (pH 8.0), 0.2% NP-40,

1 μmol/L EDTA (pH 7.6)] supplemented with protease inhibitor cocktail Complete Mini (Roche Diagnostics). After centrifugation of the homogenates (3000*g* for 10 minutes), the supernatants or serum samples were used for measurement. To activate latent TGF-β_1 to an immunoreactive form, the samples were treated with acid according to the manufacturer's instructions (R&D Systems Inc). IL-10 or IL-6 concentrations in the sera and TGF-β_1, IL-6, HO-1, or TNF-α in the lung extracts were measured using enzyme-linked immunosorbent assay (ELISA) kits (Amersham Pharmacia Biotech; R&D Systems). The minimum detectable dose was 3, 3, 16, and 5 pg/mL or 0.78 ng/mL for IL-10, TGF-β_1, IL-6, and TNF-α, or HO-1, respectively. Inter- and intraassay precision of these kits was <10%. The total protein concentrations in the lung extracts were estimated using a BCA Protein Assay kit (PIERCE). The levels of TGF-β_1, IL-6, HO-1, or TNF-α in the lung were expressed as pg per mg protein.

Cell Culture and Proliferation Assay

Human PASMCs were obtained from Clonetics Corp and grown in SmGM-2 medium (Clonetics Corp). PASMCs with a passage between 4 and 6 were used in the experiments. Cells (1×10^3 per well) were incubated in 96-well plates with serum-free Dulbecco's modified Eagle's medium and nutrient mixture F12 (DMEM-F12, Invitrogen) in an atmosphere of 5% CO_2 in the air at 37°C. A tetrazolium-based colorimetric proliferation assay (XTT assay; Cell Proliferation Kit II, Roche Diagnostics) was performed 2 days after adding tin protoporphyrin IX (SnPP; Frontier Scientific), human recombinant TGF-β_1, IL-6, or IL-10 (PeproTech Inc). The optical density between 450 and 650 nm were measured to estimate the number of viable cells.

Statistical Analysis

Data from multiple experiments are expressed as mean±SEM. Statistical analysis and correlations were performed using StatView (Abacus Concepts, Inc). Survival curves were analyzed using the Kaplan–Meier method and compared by log-rank tests. Differences in other parameters were evaluated by analysis of variance combined with Fisher test. The correlation test was used to measure the association between 2 variables. A value of $P<0.05$ was considered statistically significant.

Results

AAV Vector-Mediated IL-10 Expression Improves Survival of MCT-PAH Rats

Eight weeks after AAV-IL-10 injection, serum IL-10 concentrations were elevated in a vector dose-dependent manner (Figure 1A). We determined that injection with AAV-IL-10 (6×10^{10} g.c. per rat) significantly increased serum IL-10 levels as compared with untreated controls (184.1±47.6 versus 18.8±1.3 pg/mL, $P<0.05$, n=3 each). In contrast, injection with MCT (Figure 1A) or AAV-eGFP alone (data not shown) caused no significant change in serum IL-10 levels. Therefore, we used this dosage for all vectors in subsequent experiments. For survival analysis, the rats were injected with a lethal dose of MCT, after 4 weeks of vector injection. The survival in IL-10–transduced rats was significantly improved as compared with the eGFP-transduced rats 8 weeks after MCT injection (75% versus 0%, $P<0.01$, n=8 each; Figure 1B).

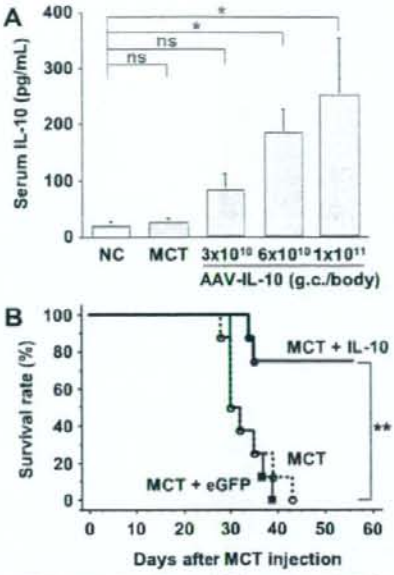

Figure 1. Adeno-associated virus (AAV) vector-mediated systemic interleukin (IL)-10 expression improves survival of monocrotaline (MCT)-induced pulmonary arterial hypertension (PAH) rats. A, In vivo IL-10 expression induced by AAV-IL-10. Serum IL-10 concentrations (pg/mL) were determined using ELISA 8 weeks after a single intramuscular injection of AAV-IL-10 into the anterior tibial muscles of 3-week-old Wistar rats. Genome copies (g.c.) per rat were as indicated. Data represent mean±SEM (n=3 animals per group, *$P<0.05$). ns indicates not statistically significant; NC, untreated controls. B, The Kaplan-Meier survival curve in MCT-PAH rats. The Wistar rats were treated with a lethal dose of MCT 4 weeks after the single intramuscular injection of HN buffer (MCT group), AAV-eGFP (MCT+eGFP group), or AAV-IL-10 (MCT+IL-10 group). n=8 animals per group, **$P<0.01$ versus MCT or MCT+eGFP groups.

Effects of IL-10 on PAH and RVH

Four weeks after MCT injection, the mPAP levels were significantly higher than those of the untreated controls (30.1±4.0 versus 20.0±2.1 mm Hg, $P<0.01$, n=5 each; Figure 2A). Treatment with AAV-IL-10 but not AAV-eGFP significantly inhibited the elevation of mPAP (22.8±1.5 versus 29.7±2.8 mm Hg, $P<0.01$, n=5 each; Figure 2A). Moreover, serum IL-10 concentrations correlated negatively with mPAP in MCT-treated rats ($r=-0.75$, $P<0.01$, n=15; Figure 2B). In contrast, this IL-10 expression caused no significant change in HR (data not shown) and mAoP (76.7±2.1 versus 74.6±6.8 mm Hg, MCT+IL-10 versus MCT+eGFP group, n=5 each). IL-10 expression also has a beneficial effect on RVH. Four-week MCT treatment significantly increased the RV/(LV+S) values as compared with the untreated controls ($P<0.01$, n=5 each; Figure 2C). Treatment with AAV-IL-10 but not AAV-eGFP inhibited MCT-induced increase of RV/(LV+S) significantly ($P<0.05$, n=5 each; Figure 2C). Furthermore, serum IL-10 concentrations correlated negatively with RV/(LV+S) in MCT-treated rats ($r=-0.57$, $P<0.05$, n=15; Figure 2D). These results indicate that sustained IL-10 expression prevented the development of MCT-induced PAH and RVH.

Effects of IL-10 on Histological Changes of the PA

Medial hypertrophy is a hallmark of pathological vascular remodeling in PAH. Four weeks after MCT injection, the medial thickness of PAs was markedly increased in the MCT-treated rats compared with untreated controls ($P<0.01$,

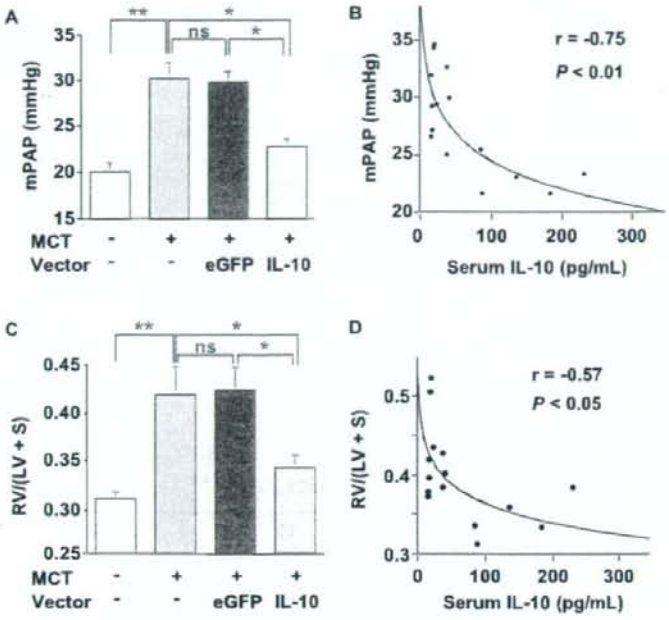

Figure 2. Effects of IL-10 on PAH and right ventricular hypertrophy (RVH). The 7-week-old Wistar rats were treated with monocrotaline (MCT) 4 weeks after vector injection. A, Statistical analysis of mean pulmonary arterial pressure (mPAP, mm Hg) determined by direct catheterization 4 weeks after MCT injection. Data represent the mean ± SEM (n=5 animals per group; $^*P<0.05$, $^{**}P<0.01$). ns indicates not statistically significant. B, Correlation between serum IL-10 concentrations and mPAP levels in the MCT-treated rats (groups: MCT, MCT+eGFP, or MCT+IL-10; n=5 animals per group; $r=-0.75$, $P<0.01$). C, Quantitative RVH analysis. The weight ratio of the right ventricle to left ventricle plus septum [RV/(LV+S)] is presented as an index of RVH (n=5 animals per group; $^*P<0.05$, $^{**}P<0.01$). D, Correlation between serum IL-10 concentrations and RV/(LV+S) in the MCT-treated rats (groups: MCT, MCT+eGFP, and MCT+IL-10; n=5 animals per group; $r=-0.57$, $P<0.05$).

n=5 each; Figure 3B, 25 to 50 μm; Figure 3C, 51 to 100 μm in external diameter). Treatment with AAV-IL-10 but not AAV-eGFP significantly inhibited the increase in percent medial thickness ($P<0.01$, n=5 each). Inflammatory cell infiltration and vascular cell proliferation are also important indicators in the progression of PA remodeling. Immunohistochemical analysis shows that treatment with AAV-IL-10 significantly decreased the number of accumulated macrophages (ED1-positive cells; $P<0.01$, n=5 each; Figure 3D) and proliferating vascular cells (PCNA-positive cells; $P<0.01$, n=5 each; Figure 3E) in the PA of MCT-treated rats as compared with treatment with MCT alone or AAV-eGFP.

Effects of IL-10 on Cytokine Expression

We analyzed pulmonary tissue and serum cytokine levels relevant to the pathogenesis of PAH. Four weeks after MCT injection, the TGF-β_1 and IL-6 levels in the MCT-treated rats were significantly higher than those of the untreated controls ($P<0.01$, n=5 each; Figure 4A and 4C). Treatment with AAV-IL-10 but not AAV-eGFP significantly inhibited the MCT-induced elevation of TGF-β1 and IL-6 levels ($P<0.01$, n=5 each). Furthermore, these levels correlated positively with the percent medial thickness in the rats with or without MCT treatment ($r=0.84$, $P<0.01$; $r=0.87$, $P<0.01$, respectively; Figure 4B and 4D).

HO-1 has been reported to mediate the antiinflammatory effects of IL-10.[24] Treatment with AAV-IL-10 but not AAV-eGFP or MCT alone significantly increased the lung HO-1 levels as compared with untreated controls ($P<0.05$, n=5 each, Figure 4E). In addition, HO-1 levels correlated negatively with IL-6 levels in MCT-treated rats ($r=-0.85$, $P<0.01$; Figure 4F). In contrast, serum IL-6 levels positively correlated with lung IL-6 levels ($r=-0.69$, $P<0.01$; Figure 4G). Although the lung TNF-α levels significantly increased in MCT-treated rats compared with untreated controls, IL-10 expression caused no change in the lung TNF-α levels (Figure 4H).

Effects of IL-10 on PASMC Proliferation

To determine whether IL-10 directly inhibits PASMC proliferation, we performed an in vitro colorimetric XTT assay using cultured human PASMCs. Treatment of PASMCs with SnPP, which inactivates HO-1, and treatment with TGF-β_1 or IL-6 dose dependently promoted cell proliferation (n=4 each, $P<0.05$; Figure 5A through 5C). Treatment with IL-10 alone had no significant effect on PASMC proliferation (Figure 5D). On the other hand, pretreatment with IL-10 significantly inhibited PASMC proliferation induced by SnPP or TGF-β_1 (n=4 each, $P<0.05$; Figure 5E) but not that induced by IL-6.

Discussion

The present study demonstrates that IL-10, delivered by an intramuscular injection of an AAV1 vector, prevented the development of MCT-PAH in rats. Systemic IL-10 expression also improved survival in rats and prevented the development of RVH and medial hypertrophy of PA. IL-10 also reduced macrophage accumulation, vascular cell proliferation, and pulmonary tissue levels of TGF-β_1 and IL-6, all of which play pivotal roles in progression of PA remodeling. Further, IL-10 enhanced HO-1 levels in the lung. Thus, IL-10 exerts multiple preventive effects on inflammatory and proliferative PA remodeling (Figure 6).

Blockade of a single proinflammatory signaling pathway by IL-1 or monocyte chemoattractant protein-1 attenuates PA remodeling.[25,26] However, the prosurvival effects of antiinflammatory molecules on PAH animals have not been re-

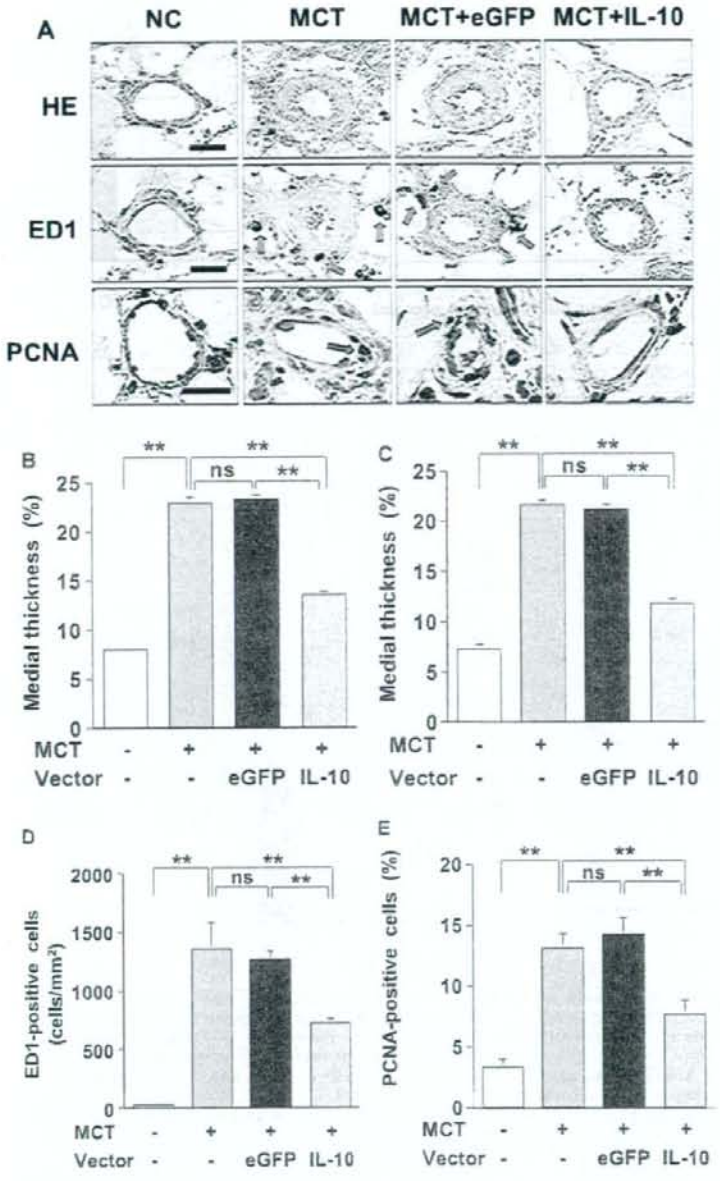

Figure 3. Antiinflammatory and antiproliferative effects of IL-10 on the remodeled pulmonary artery (PA). The 7-week-old Wistar rats were treated with MCT 4 weeks after vector injection. Representative cross-sectional views of the peripheral PAs stained with HE or immunohistochemistry (ED1 or PCNA) 4 weeks after MCT treatment (A; original magnification ×1000, Scale bar=20 μm). Blue arrows indicate ED-1–positive cells and red arrows, PCNA-positive cells. Quantification of percent medial thickness for vessels 25 to 50 μm (B) and 51 to 100 μm (C) in external diameter. Quantitative analysis of the number of perivascular macrophages (ED-1–positive cells, D) and proliferating vascular cells (PCNA-positive cells, E). Data represent mean SEM ($n=5$ animals per group, $^{**}P<0.01$). ns indicates not statistically significant.

ported. Evidence of right heart failure is involved in the mortality of MCT-PAH rats. In this study, all rats treated with a lethal dose of MCT exhibited symptoms of right heart failure such as pleural effusion and body weight decrease. In the setting of severe PAH and right heart failure, cytokine networks may orchestrate disease progression. Thus, blockades of multiple inflammatory signals might be responsible for the prosurvival effect of IL-10.

IL-10 has gained significant attention because of its suppressive influence on inflammatory and proliferative vasculopathy. The IL-10 receptor is expressed on vascular smooth muscle cells (VSMCs). IL-10 inhibits inflammation and VSMC proliferation in arterial remodeling after balloon injury or transplant rejection.[12,13] Consistent with previous studies using MCT-PAH,[6,7] we demonstrate that increased levels of TGF-β_1 and IL-6 are related to PASMC proliferation and PA remodeling progression. Although treatment with IL-10 alone caused no significant effects on PASMC proliferation,[27] IL-10 significantly inhibited the lung TGF-β_1 expression and TGF-β_1-induced PASMC proliferation. TGF-β_1 enhances PASMC proliferation of idiopathic PAH patients but not that of normal subjects or secondary PAH patients.[28]